Biochimica et Biophysica Acta 1818 (2012) 1807–1822

Contents lists available at SciVerse ScienceDirect

Biochimica et Biophysica Acta

journal homepage: www.elsevier.com/locate/bbamem

Review

Voltage-dependent conformational changes in connexin channels ☆

Thaddeus A. Bargiello [a,*], Qingxiu Tang [a], Seunghoon Oh [b], Taekyung Kwon [a]

[a] Dominic P. Purpura Department of Neuroscience, Kennedy Center, Albert Einstein College of Medicine, Bronx, NY 10461, USA
[b] Department of Physiology, College of Medicine, Dankook University, Cheonan City, 330-714, Republic of Korea

ARTICLE INFO

Article history:
Received 19 May 2011
Received in revised form 9 September 2011
Accepted 17 September 2011
Available online 24 September 2011

Keywords:
Ion channel
Gap junction
Voltage-dependent gating
Cadmium metal-bridge
Structure–function
Molecular dynamics

ABSTRACT

Channels formed by connexins display two distinct types of voltage-dependent gating, termed V_j- or *fast-gating* and *loop-* or *slow-gating*. Recent studies, using metal bridge formation and chemical cross-linking have identified a region within the channel pore that contributes to the formation of the loop-gate permeability barrier. The conformational changes are remarkably large, reducing the channel pore diameter from 15 to 20 Å to less than 4 Å. Surprisingly, the largest conformational change occurs in the most stable region of the channel pore, the 3_{10} or parahelix formed by amino acids in the 42–51 segment. The data provide a set of positional constraints that can be used to model the structure of the loop-gate closed state. Less is known about the conformation of the V_j-gate closed state. There appear to be two different mechanisms; one in which conformational changes in channel structure are linked to a voltage sensor contained in the N-terminus of Cx26 and Cx32 and a second in which the C-terminus of Cx43 and Cx40 may act either as a gating particle to block the channel pore or alternatively to stabilize the closed state. The later mechanism utilizes the same domains as implicated in effecting pH gating of Cx43 channels. It is unclear if the two V_j-gating mechanisms are related or if they represent different gating mechanisms that operate separately in different subsets of connexin channels. A model of the V_j-closed state of Cx26 hemichannel that is based on the X-ray structure of Cx26 and electron crystallographic structures of a Cx26 mutation suggests that the permeability barrier for V_j-gating is formed exclusively by the N-terminus, but recent information suggests that this conformation may not represent a voltage-closed state. Closed state models are considered from a thermodynamic perspective based on information from the 3.5 Å Cx26 crystal structure and molecular dynamics (MD) simulations. The applications of computational and experimental methods to define the path of allosteric molecular transitions that link the open and closed states are discussed. This article is part of a Special Issue entitled: The Communicating junctions, composition, structure and characteristics.

Contents

☆ This article is part of a Special Issue entitled: The Communicating junctions, composition, structure and characteristics.

* Corresponding author. Tel.: +1 718 430 2575.
E-mail address: ted.bargiello@einstein.yu.edu (T.A. Bargiello).

0005-2736/$ – see front matter © 2011 Elsevier B.V. All rights reserved.
doi:10.1016/j.bbamem.2011.09.019

1. Introduction

Different subsets of connexin proteins are expressed in almost all mammalian tissues and organ systems [1] where they form intercellular gap junction channels with diverse physiological properties. Gap junction channels are formed by the head-to-head docking of two hemichannels in adjacent cells to provide a direct communication pathway for intercellular electrical and chemical signaling. This signaling plays a vital physiological function in many organs including heart and brain, where gap junctions form electrical synapses; and in non-excitable tissues such as liver and pancreas, where they synchronize cellular activity and secretion. It has been proposed that Cx26 gap junctions in cochlear epithelium mediate IP_3 transfer between supporting cells essential to sustaining the endolymphatic potential and high K^+ concentration required for signal transduction and cellular homeostasis [2]. Subsets of hemichannels not docked with apposed hemichannels mediate plasma membrane currents and molecular flux in native tissues and exogenous expression systems [3–6]. We term these, *undocked* or *unapposed* hemichannels. The open probability of both intercellular and undocked connexin channels is regulated by extrinsic parameters including voltage, pH, and [Ca^{2+}] and by the intrinsic properties of the specific connexin isoforms expressed in the tissue. Recent studies indicate that undocked hemichannels have important physiological functions in health and disease. For example, misregulation of Cx26 hemichannels results in severe skin disorders that can be fatal as a consequence of secondary infection of skin lesions [7–9].

The solution of a Cx26 gap junction structure at 3.5 Å by X-ray crystallography [10] has greatly advanced our understanding of the structure–function relations of connexin channels. However, it should be kept in mind that the structure represents a single experimental determination and because it is a moderate to low resolution structure, there is a degree of uncertainty surrounding side chain positions. Therefore, while structure–function correlates can be inferred from the crystal structure, they should be viewed with a degree of caution. Recently the crystal structure has been refined with molecular dynamics (MD) simulations [11]. The resulting "average equilibrated structure" appears to more closely correspond to the structure of the open Cx26 hemichannel than does the crystal structure. This review will focus on recent studies of voltage-dependent conformational changes in connexin channel structure, primarily in terms of insights gained from the crystal structure and MD simulations. Mechanisms and molecular determinants of voltage gating have been reviewed recently [12–14] and no attempt is made to provide an exhaustive review of available literature.

Connexins form large pore ion channels. The minimum pore diameter of the open channel, determined by functional studies [15, 16] is in the range of 12–15 Å. In contrast, the minimum pore diameter of the fully closed (non-conducting) channel must be less than the diameter of fully hydrated K^+ (6.62 Å) and Cl^- (6.64 Å) ions [17], and perhaps as small as 3.5 Å if one considers the van der Waals diameters of dehydrated K^+ (5.5 Å) and Cl^- (3.5 Å). The challenge from a thermodynamic perspective is to understand how such a large conformational change is accomplished. Are the conformational changes highly focal, being restricted to a specific location within the pore or are they global, i.e. changes involving multiple channel domains? Since the rate of transition is a function of the energy barrier between states [18], the question is in essence one concerning the height and width of the energy barrier separating open and closed states. The path linking open and closed states will follow the lowest energy path of the molecular transition(s) that interconnect the two. It seems reasonable to expect that the height of the energy barrier for a highly focal conformational change will be lower than that for a large global conformational change in channel structure.

2. Conformational changes mediated by extracellular calcium and pH

Studies of conformational changes in connexin channels have used a variety of methods and preparations. The first reports of conformational changes in gap junctions in response to extracellular Ca^{2+} in the absence of applied voltage were the cryo-EM studies of Unwin and co-workers [19–21]. They reported that low concentrations of Ca^{2+} (accomplished by differential dialysis) resulted in small cooperative rearrangements of rat liver gap junctions that were best explained by rigid body rotational pivoting and tilting of the six channel subunits. This led to a "camera iris" shutter model of gating reviewed by Bennett et al. [22]. More recent studies, using atomic force microscopy (AFM) [23], reviewed by Sosinsky and Nicholson [24], showed that 0.5 mM Ca^{2+} decreased the diameter of the extracellular entrance of Cx26 hemichannels from ~15 Å to ~6 Å. Conformational changes were also observed at the intracellular entrance of the pore, but these were more difficult to interpret as a consequence of the flexibility of the cytoplasmic surface, a feature subsequently confirmed by calculation of the temperature factors of the Cx26 crystal structure [10] and MD simulation [11]. More recently, Lal and co-workers reported Ca^{2+} induced conformational changes at both the intracellular and extracellular entrance to Cx40 channels [25]. The original EM and subsequent AFM studies suggest that Ca^{2+} gating involves substantial conformational changes of the entire channel. If so, one expects the enthalpic barrier that separates the open and closed states driven by Ca^{2+} concentration to be substantial, if the entropy of the open and closed states are similar. Notably, comparable structural changes determined by AFM were not induced by up to 2 mM Mg^{2+} in Cx26 hemichannels [23, 24]. An important question is whether the effects of Ca^{2+} observed in structural studies result from the direct action of Ca^{2+} on the channel or if the effects are indirect, mediated by changes in membrane fluidity. It has been reported that Ca^{2+} has a more pronounced effect on phosphatidylserine containing membranes than does Mg^{2+} [26] (see also [27, 28]).

The relation between conformational changes determined by structural studies and those determined electrophysiologically in response to voltage need to be examined further. One issue is the structural implication of the differential sensitivity of channels to Ca^{2+} and Mg^{2+} determined in structural studies (such as AFM) compared to the sensitivity of voltage induced conformational changes to divalent cations. In other words, are the conformational changes induced by Ca^{2+} and Mg^{2+} by themselves (chemical gating) and in combination with voltage (modulation of voltage-gating) the same?

2.1. Modulation of voltage-gating by divalent cations

Ca^{2+} and Mg^{2+} have been reported to modulate voltage-dependent loop-gate but not V_j-gate closure (see following section for definition of V_j- and loop-gating) of Cx46 hemichannels by stabilizing the closed conformation by interaction with an extracellular site outside the channel pore [29] (see also [30] for Cx32 hemichannels). This contrasts a mechanism of Ca^{2+} regulation of Cx37 hemichannels that is based on voltage-dependent open channel block [31] that would occur in the absence of conformational change. The Cx46 results suggest that the effect of Ca^{2+} requires closure of loop-gates by voltage. The structural studies, which are performed in the absence of an electrical field, suggest that Ca^{2+} induces conformational changes that are voltage independent.

Furthermore, as described later, voltage-dependent loop-gate closure in the chimeric Cx32*43E1 hemichannel does not appear to produce substantial narrowing of the extracellular entrance to the channel pore in contrast to AFM studies of Cx26 and Cx40 closed by Ca^{2+}. The difference suggests that the conformational changes reported in structural studies in response to Ca^{2+} may differ from those occurring during voltage-dependent gating.

Voltage-dependent closure of other connexin hemichannels expressed in *Xenopus* oocytes are known to be modulated by $[Ca^{2+}]_o$, including Cx26 [8, 32], but the sensitivity of Cx26 hemichannel voltage-gating modulation by Mg^{2+} has not been reported. Modulation of voltage-gating of Cx46 hemichannels is approximately 10 times more sensitive to Ca^{2+} than Mg^{2+} [29, 33] while that of Cx50 hemichannels is strongly dependent on Ca^{2+} but weakly sensitive to Mg^{2+} [34]. Cx32*43E1 hemichannels are ~2 times more sensitive to external Ca^{2+} than Mg^{2+} (Bargiello lab, unpublished observations). The differential sensitivity of different connexin hemichannels to Ca^{2+} and Mg^{2+} suggests that the position and or amino acid composition of the interacting site(s) differ among hemichannels. Comparison of Ca^{2+} and Mg^{2+} coordination in proteins have been investigated, for example [35], and may provide valuable information relevant to the differential sensitivity of connexins to divalent cations.

2.2. pH gating

Studies by Delmar and colleagues of gating of Cx43 channels by pH suggest a specific conformational gating mechanism: the "particle-receptor" model [36] that leads to channel closure at low pH. This model is based on a number of experimental methods including; structure–function inferences drawn from mutational analyses, interactions measured by biophysical methods including translational diffusion rates and surface plasmon resonance (SPR) and structural studies of CT and CL peptides by NMR [37–40]. In this model, the cytoplasmic terminal domain (CT) of Cx43 acts as a "mobile" particle that interacts with a receptor contained within the cytoplasmic loop (CL) to effect pH gating. It is not clear if channel closure occurs by the CT directly blocking the pore or by the stabilization of the pH closed state. In contrast, pH gating of Cx46 hemichannels appears to involve the direct action of H^+ ions close to the intracellular entrance of the channel pore [41]. AFM studies of the CT of Cx43 channels were interpreted to support a "ball and chain" type model for hemichannel conformational changes [42] in that the CT was shown to be flexible and not closely associated with other domains in the open state.

Conceptually analogous models to the Cx43 pH-gating model were proposed to explain voltage-gating of Cx43 and Cx40 channels [37, 43]. Based on electrophysiological studies of site directed mutations, Revilla et al. [44] proposed that some aspects of Cx32 voltage-gating arise from the movement of the CT into the channel pore. On the basis of structural studies of wild type and the Cx26M34A mutation, Oshima and co-workers [45–47] proposed a "gating plug" model in which a voltage-driven change in the position of the flexible N-terminal domain (NT) of Cx26 within the channel pore creates a permeability barrier [10, 47]. In the simplest case, the common feature shared by these gating models is that they appear to only require conformational changes restricted to a distinct flexible region of the channel. At first glance, it would appear that such transitions would not require crossing large thermodynamic barriers, at least for channel closure, if the mechanism involved the movement of a freely mobile protein domain to act as a blocking particle. The particle-receptor mechanism could have a large energy barrier if, for example, movement of the particle to its binding site was electrostatically or sterically constrained, or if the receptor domain was required to undergo a conformational (allosteric) change prior to particle binding. In the latter case, the particle could be viewed as stabilizing a conformational state. These possibilities are discussed further in Section 5.

3. Voltage-gating of connexin channels

Voltage is an important parameter regulating the opening and closing of all connexin channels. In principle, intercellular channels can be sensitive to two orientations of applied voltage, 1) the voltage difference between the cytoplasm and the extracellular space, the inside–outside voltage, termed V_{i-o} or V_m and 2) the voltage difference between the cytoplasms of the two cells, the trans-junctional voltage, termed V_j. V_j sensitivity depends solely on the difference in the potential of two coupled cells and is independent of the absolute membrane potential of each cell. For example, the V_j established by holding one cell at +50 and a coupled cell at −50 mV elicits the same voltage-dependent response as that created by holding one cell at 0 mV and the second cell at −100 mV in spite of differences in absolute membrane potential in the two cases. These features of connexin voltage gating have been reviewed by Bargiello and Brink [14].

Most gap junctions formed by connexins display sensitivity only to V_j, whereas those formed by the distantly related innexin gene family can display both strong V_j- and V_{i-o}-dependence [48]. The studies of Harris et al. [49], using vertebrate gap junctions sensitive to only V_j, established that V_j-dependence was an intrinsic hemichannel property. Each hemichannel was shown to contain a voltage sensor and gate that operates in series with the same elements located in the apposed hemichannel. A second major concept established by this study, based on the observation of contingent gating, was that the transjunctional voltage sensor would most likely reside in the channel pore. Positioning of the voltage sensor in the channel pore is required to allow sensitivity to only V_j [13, 14]. Verselis et al. [48] proposed that the V_{i-o} sensor would be located in the extracellular loops of invertebrate gap junctions (in the region of the intercellular gap), allowing it to move in response to V_{i-o} but not V_j. Note that the application of V_j in this case would activate both V_j and V_{i-o} (also termed V_m) gates as application of V_j must change membrane potential.

The demonstration that connexin hemichannels could open in the plasma membrane of *Xenopus* oocytes [50] when unapposed by another hemichannel marked a turning point in studies of the structure–function relations of connexin channels. This property expanded the range of experimental techniques that could be applied to the study of connexins, notably the application of single channel methods that provided access to both the intracellular and extracellular entrance to the channel pore. These studies lead to the identification of:

1) Two distinct voltage-gating mechanisms, termed "loop"- or "slow"-gating, and "V_j"- or "fast"-gating [51].
2) The molecular determinants and stoichiometry of V_j-gating polarity [52–54].
3) The identification of the location of the loop-gate permeability barrier inferred from accessibility studies [55].
4) The identification of amino acids in TM1/E1 region that form at least a portion of the loop-gate permeability barrier [34, 56].
5) The molecular determinants of charge selectivity of Cx46 and Cx32*43E1 [54, 57].
6) The pore lining domains of connexin channels [58, 59] with the substituted cysteine accessibility method [60]. The results of these studies indicated that hemichannel pore was formed in part by residues located in the first transmembrane domain TM1, the first extracellular loop (E1) and the N-terminus (NT). The Cx26 crystal structure is in agreement with these findings. Some experimental work suggests that TM3 lines the pore of gap junctions [61], which led to the suggestion that the structure of the channel pore changes with the formation of an intercellular channel. However, it is difficult to reconcile a role for TM3 in pore formation with the crystal structure of the Cx26 gap junction and by the formation of a portion of the loop-gate permeability barrier at the TM1/E1 boundary. A large scale reorganization of the packing order of transmembrane helices and breaking and reforming

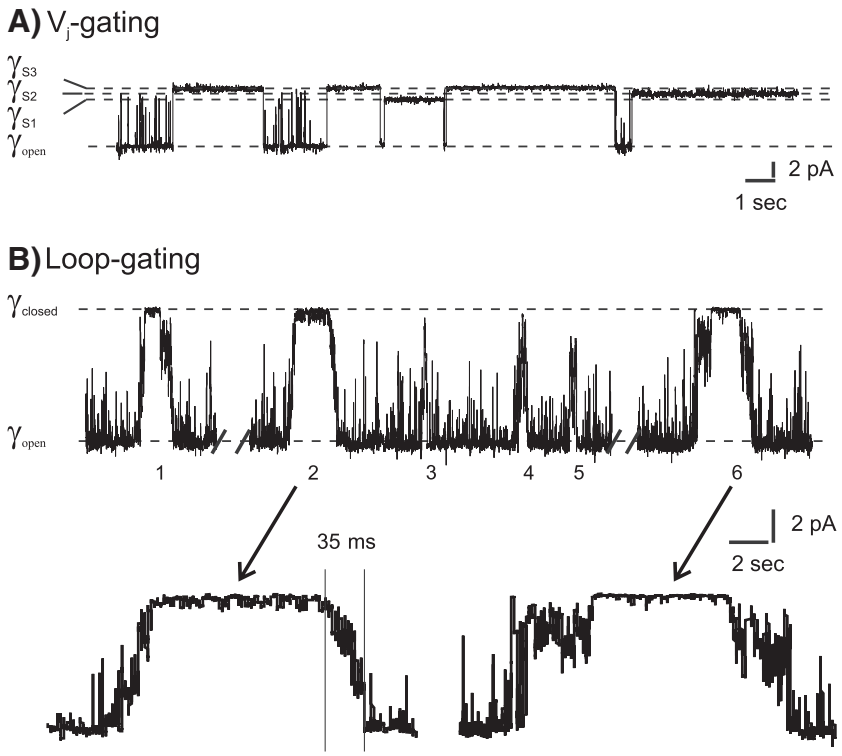

Fig. 1. Single channel records of an undocked Cx32*Cx43E1 hemichannel in *Xenopus* oocyte. (A) Outside-out record of a single channel illustrating closures by V_j-gating to three substates at a holding potential of −100 mV. (B) Cell-attached recording of a single wild-type channel illustrating six loop-gating events at a holding potential of −70 mV. Note the slow time course of the transitions indicated for events 2 and 6 in the lower panel of B and that not all transitions necessarily lead to full channel closure, as indicated by the partial closure of events 3–5.

interactions with surrounding lipid resulting from hemichannel docking is unlikely to be energetically feasible.

From a biophysical and structure–function perspective, voltage gating is most effectively studied in undocked hemichannels where the operation of each gate (loop and V_j) can be directly observed. This circumvents the complication of identifying the individual contribution of four gates (2 V_j,- 2 loop-gates) operating in series that occurs in intercellular channels [62, 63]. While this is possible, it requires inferences based on mathematical models of the intercellular channels rather than direct observation of gating events.

The question then is how closely the properties of a hemichannel correspond to those of intercellular channels. Most studies indicate that there is close correspondence. Srinivas et al. [64] reported that several properties of Cx46 and Cx50 gap junction channels, including unitary conductance, sensitivity to pharmacological agents, and voltage-gating can be explained by the properties of undocked Cx46 and Cx50 hemichannels. Ebihara et al. [65] reached the same conclusion in earlier studies of the voltage gating of Cx46 and Cx56 channels as did Beahm and Hall [66] for Cx50 channels. Similar principles are evident in studies of voltage gating and current rectification of Cx26 and Cx32 [67–69], where the properties of homotypic and heterotypic intercellular channels can be explained in terms of the properties of their component hemichannels. Together, these reports support the view that the structure and function of connexin hemichannels is largely conserved when they function individually as undocked hemichannels or in series as intercellular channels. The current view is that formation of an intercellular channel can modulate the expression of voltage-dependence (an intrinsic hemichannel property) but pairing of two hemichannels does not create novel gating mechanisms.

Connexin channels display at least two distinct voltage gating processes, termed *loop-* or *slow-gating* and *V_j-* or *fast-gating* that are defined by how they appear in single channel records [51, 64, 69]. These two processes were first described in insect cell lines [70] now known to be formed by innexins, a family of proteins with no sequence homology to connexins. In connexin channels, V_j or fast-gating corresponds to events in which the channel closes to distinct subconductance states with a time course that cannot be resolved in patch clamp recordings (Fig. 1A). The term V_j-gating was adopted to reflect the correspondence between the entry of the hemichannel into substates in single channel recordings and a minimal conductance, G_{min}, in macroscopic recordings of intercellular channels in response to V_j. Others use the term fast-gating rather than V_j-gating to describe the kinetics of current relaxations observed in macroscopic recordings. Bukauskas and Verselis [13] discuss the relationship between speed of gating transitions and gating kinetics. The polarity of V_j-gating differs among connexin channels formed by Cx26 and Cx32 [67], e.g. the V_j-gate of Cx32 hemichannels closes as the inside potential becomes more negative (hyperpolarization), while in Cx26 hemichannels, the V_j-gate closes as the inside potential becomes more positive (depolarization). Cx43 and Cx40 intercellular channels display a form of substate gating that has also been termed fast gating. This terminology was initially based on the kinetics of current relaxation [44] rather than the rapid time course of the gating transition. As described later, this form of gating appears to involve and interaction between the CT and CL of these connexins, and may represent a different fast-gating mechanism than described for Cx32, Cx26 and Cx46 channels.

Loop-gate closure is favored at inside negative potentials in all connexin hemichannels examined to date. In single channel recordings, loop-gating transitions between open and fully closed state pass through multiple metastable intermediate states [51]. This is illustrated in Fig. 1B for the undocked chimeric Cx32 hemichannel (Cx32*Cx43E1) first described by Dahl and co-workers [71] and characterized at the single channel level by Oh et al. [69]. It was proposed that the intermediate states reflect conformational changes by each component connexin monomer in the hemichannel [51], but this has not been confirmed. Transitions connecting the intermediate states are rapid and are not resolved in patch clamp recordings.

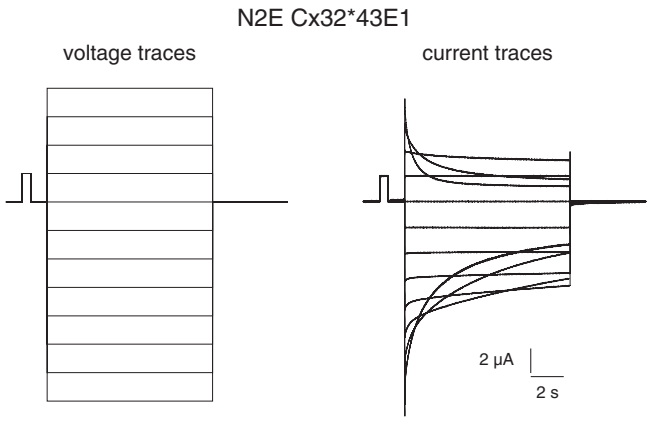

Fig. 2. Macroscopic recording of N2E Cx32*Cx43E1 hemichannel in *Xenopus* oocytes. Currents shown in the panel on the right were elicited by voltage steps from 0 mV to 40 through −70 mV in 10 mV increments shown in the voltage traces in the left panel. Current relaxations at inside positive potentials (depolarization) result from V_j-gating while those at inside negative potentials (hyperpolarization) result from loop-gating. The N2E substitution reverses the polarity of V_j-gating of the wild type Cx32*Cx43E1 hemichannel. In the wild type channel, current relaxations are only observed with hyperpolarization (not depicted).

The dwell time in any given intermediate state is voltage dependent, decreasing markedly with increasing hyperpolarization. At intermediate voltages, the transition from the open to fully closed channel has an appreciable time constant, in the millisecond range, giving the appearance of a "slow" gating event (see [13] for review and Fig. 1.B). The voltage-dependence of loop-gating favors hemichannel closure at the resting membrane potential of most cells, and thus, in combination with extracellular [Ca^{2+}] maintains hemichannels in a closed state prior to the formation of intercellular channels. As described above, divalent cations are believed to stabilize the closed conformation.

Similar appearing slow events (loop-gating) are also observed in Cx32, Cx43, Cx45 and Cx40 intercellular channels as well as fast transitions (V_j-gating) [13, 15, 72, 73]. Thus, it appears that the loop-gating mechanism operates in both undocked hemichannels and intercellular channels in spite of constraints imposed on the position of the extracellular loops that are required for intercellular channel formation. While this observation does not exclude the possibility that the two extracellular loops participate in loop-gating, it suggests that they may not play a major role in the conformational changes required to close the channel.

While the kinetics of V_j-gating and loop-gating have not been extensively studied in terms of kinetic models and their thermodynamic implications, the long time constants obtained from the relaxation of macroscopic currents of undocked hemichannels expressed in *Xenopus* oocytes strongly suggest that the energy barrier separating the open and both the V_j- and the loop-gate closed states is high. For example, the time constants of the current relaxations of a N2E–Cx32*43E1 hemichannel shown in Fig. 2 are in the order of seconds (tau for the closure of V_j-gates is ~1.25 s at 40 mV, tau for closure of loop-gates is ~3.5 s at −70 mV). Recall that in this hemichannel, current relaxations observed at inside positive potentials result from closure of V_j-gates, while current relaxations observed at inside negative potentials result from closure of loop-gates. The channel is fully open at intermediate membrane potentials around 0 mV (Fig. 2). This indicates that the free energy of the open state is much lower than that of the closed states in the absence of an applied voltage. Consequently, voltage is believed to effect channel closure by the destabilization of the open state and the stabilization of the closed states. The presence of a large energy barrier is supported by kinetic analyses reported for other connexin channels (see [49, 74–76] for examples). The time constants for different connexins vary from hundreds of milliseconds to seconds. For comparison, the activation energies of the final transitions that link the open and closed states of voltage-gated Shaker K^+ and squid giant axon Na^+ channels can be as high as ~12–15 kcal/-mol with substantial enthalpic and entropic components [77–79]. The time constants of these transitions are in the ms range, i.e. at least one or two orders of magnitude faster than the time constants reported for connexin channels.

It is important to keep in mind that two components must be considered in the kinetics of channel closure. One is the latency to the gating event, the second is the kinetics of the actual gating transition. Both may be voltage-dependent. That is, the probability that a gating event is initiated is voltage-dependent; indicating that the probability that the channel samples a conformation permissive to the transition is increased by the addition of energy to the system provided by voltage. For a multistep gating process such as loop-gating, the time spent in each of the intermediate "metastable" states is a function of the energy provided by voltage to surmount the energy barrier separating the intermediate states.

4. Conformational changes associated with loop-gate closure

A number of different methods have been applied to the study of voltage-dependent conformational changes of ion channels. These include spectroscopic methods, such as fluorescence quenching, FRET and LRET. These are reviewed in terms of potassium channel gating by Bezanilla [80, 81] and their use in defining the structure of the closed state of K^+ channels is described by Pathak et al. [82]. Other methods include the formation of metal bridges [83], disulfide bonds [84], and chemical crosslinking [56] as molecular rulers to establish the proximity relations between substituted residues. A comprehensive discussion of Cd^{2+} thiolate metal bridge formation as applied to the study of K^+ channels is provided by Yellen [85]. Of these, metal bridge formation, disulfide bond formation and chemical crosslinking have proved most successful in determining the conformation of the loop-gate closed state of Cx32*43E1 and Cx50 hemichannels [34, 56].

4.1. The formation of Cd^{2+} thiolate metal bridges

The molecular geometry and energetics of Cd^{2+} thiolate interactions are well established. Cadmium is a group IIB transition metal with the electronic configuration [Kr]5s04d10. It is a highly polarizable, soft ion that forms stable complexes with soft donor atoms (S≫N>O) with a preferred coordination number of 4 reflecting its electronic configuration (i.e. the outer shell of Cd^{2+} can accommodate 8 electrons, 2 from the outer shell of each thiolate group). The stabilities of Cd^{2+}–cysteine complexes are highly dependent on the number of participating thiolate groups. A tetradentate complex in which a single Cd^{2+} interacts with four cysteine residues is significantly more stable, i.e. has lower dissociation constant (K_d) or higher stability constant than do bidentate complexes [86, 87].

In a survey of protein crystal structures, Dokmanic et al. [88] reported that tetradendate coordination of Cd^{2+} by cysteine most often results from the tetrahedral organization of four cysteine-S atoms coordinated to one central Cd^{2+}. In this geometry, the Cd—S bond length is ~2.5 Å, the S—Cd—S bond angle is ~110° and sulfur atoms are separated by 4 Å (Fig. 3A). Cd^{2+} coordination can also adopt an octahedral geometry with two water molecules participating when the four cysteine sulfhydryl groups are arranged in a plane [89]. In this geometry the sulfur atoms of adjacent cysteine residues are separated by 3.5 Å (Fig. 3B). Bidentate coordination of Cd^{2+} with 2 cysteine residues in solution may also favor a tetrahedral geometry in which the two missing cysteine residues are replaced with 2 water molecules [90]. Alternatively, a less stable bidentate site can be formed by two cysteine residues separated by ~5 Å, i.e. twice the 2.5 Å optimal distance for the S—Cd interaction, if, for example steric factors reduce the access of water to the coordination site preventing the adoption of a tetrahedral geometry.

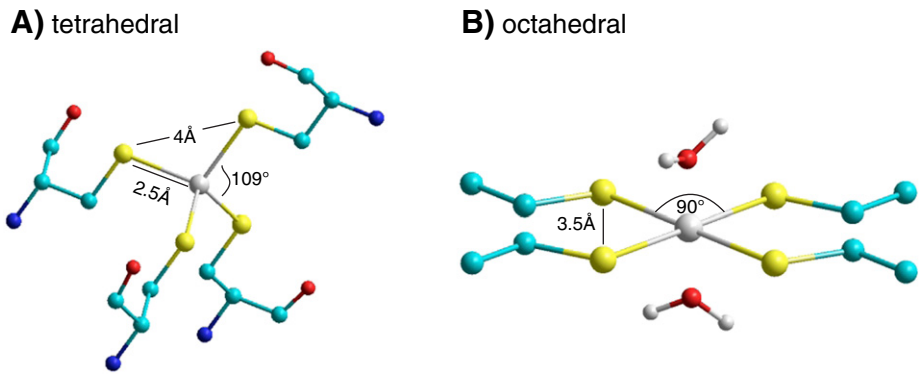

Fig. 3. Coordination geometries of tetradentate cysteine–Cd^{2+} metal bridges. (A) Tetrahedral coordination geometry showing the Cd^{2+}—S bond distance of 2.5 Å and S—C^{d2+}—S bond angle of 109°. All S atoms are separated 4 Å. (B) Planar octahedral geometry, in which the S—Cd^{2+}—S bond angle is 90° and the distance separating all S atoms is 3.5 Å. Only the cysteine side chains are shown. The positions of 2 water molecules that participate in the coordination of Cd^{2+} (white atom) are shown. Sulfur atoms are yellow spheres, carbon atoms are blue spheres, oxygen atoms are red spheres, nitrogen atoms are blue spheres.

Because the binding energy of cysteines for Cd^{2+} is very sensitive to changes in distance, movement of cysteines during gating should introduce a strong energetic bias in favor of a gating state that optimizes the coordination geometry. If cysteines adopt a spatial configuration capable of Cd^{2+} coordination, then application of Cd^{2+} will stabilize the channel in the state that allows the lowest energy Cd^{2+}–cysteine geometry. This is illustrated by considering the state diagrams shown in Fig. 4 for a channel that transits between an open and a closed state in a voltage dependent manner, as represented by the rate constants $K_1(v)$ and $K_{-1}(v)$. If the closed state "C" forms a Cd^{2+} binding site, then application of Cd^{2+} would "drive" the equilibrium to the right, by reducing the rate of channel opening. This would favor channel residency in the closed, Cd^{2+} bound state C* (Fig. 4A). The decrease in the rate constant of channel opening is determined by the binding affinity of Cd^{2+} to the coordination site. In macroscopic recordings, such a shift in kinetic equilibrium will result in 1) a decrease in current; reflecting increased channel occupancy in the closed states, and 2) a faster time constant of channel closure in the presence of Cd^{2+}; reflecting stabilization of the closed state by Cd^{2+}. Alternatively, if the open state "O" forms a Cd^{2+} binding site, then the application of Cd^{2+} would drive the equilibrium to the left, into the open Cd^{2+} bound state O* (Fig. 4B). This would result in slowing the kinetics of channel closure in macroscopic recordings. Lock of the channel in a transition state would be expected to slow the kinetics of both channel opening and closure (not illustrated).

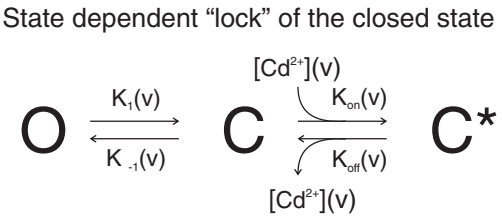

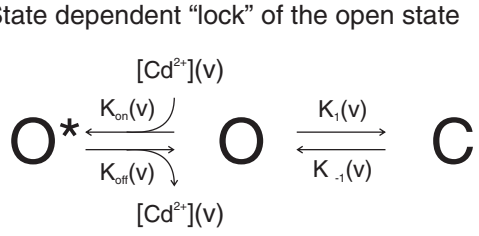

Fig. 4. State diagrams illustrating the effect of Cd^{2+} coordination on a voltage dependent two state model. (A). Cd^{2+} coordination to a binding site created only when the channel adopts the closed conformation. Binding of Cd^{2+} to the site drives the equilibrium to the right, locking the channel in the closed Cd^{2+} bound state designated at C*. (B) Cd^{2+} coordination to a binding site created when the channel adopts the open conformation. Binding of Cd^{2+} to the site drives the equilibrium to the left, locking the channel in the open Cd^{2+} bound state designated as O*. The rate constants of voltage dependent transitions between the open O and closed state C are represented as $K_1(v)$ and $K_{-1}(v)$. The voltage dependence of Cd^{2+} block [91] is represented by the term $[Cd^{2+}](v)$. The potential voltage dependence of "unblock" [92] representing the effect of voltage on the stability of bound Cd^{2+} is represented by the terms $K_{on}(v)$ and $K_{off}(v)$.

The local concentration of Cd^{2+} at the binding site can be voltage-dependent (depicted as $[Cd^{2+}](v)$), if the site is within the pore and therefore within the voltage field; hyperpolarization would favor Cd^{2+} entry from the extracellular side, while depolarization would oppose Cd^{2+} entry (see Woodhull [91]). Thus, a channel closed by hyperpolarization would appear to have a higher affinity for Cd^{2+} than a channel closed by depolarization, owing to a higher effective concentration of Cd^{2+} at the binding site than in free solution. The Cd^{2+} binding affinity itself may also be voltage dependent, in that large voltages may destabilize the binding (coordination) of Cd^{2+} to the site formed by the cysteine residues. This is conceptually equivalent to "relief" of ionic conductance block by voltage as described by French and Wells [92].

4.2. Metal bridge formation and chemical crosslinking of substituted cysteines in the TM1/E1 segment

Recently, we reported that the loop-gate permeability barrier is formed by the narrowing of the channel pore formed by the segment bounded by residues 40–50 in a chimeric Cx32 undocked hemichannel [56]. This channel, designated as Cx32*Cx43E1 (abbreviated to 43E1), replaces the first extracellular loop (residues 41–70) with the corresponding Cx43 sequence. This chimera expresses membrane currents when not docked to another hemichannel [71]. Channel closure by both the loop-gate and the V_j-gate is favored at inside negative potentials in the 43E1 hemichannel (Fig. 1) but the polarity of V_j-gating can be reversed by placement of a negative charge at the either the 2nd (N2E, see Fig. 2), 4th (T4D) and 5th (G5D) positions [52, 53, 69].

The Cx32*43E1 hemichannel provides several advantages in studies whose goal is to establish conformational changes resulting from voltage-dependent loop and/or V_j-gating by metal bridge formation. Loop-gating and V_j-gating events are readily distinguished. The chimera and polarity reversing mutation N2E have little endogenous sensitivity to Cd^{2+} (only small reduction in currents are observed when $[Cd^{2+}]>100$ μM), in contrast to Cx46 hemichannels, which display substantial reductions in current with 1–10 μM Cd^{2+} (Kwon and Bargiello, unpublished). The polarity of V_j-gating can be reversed by substitution of negative charge in the NT without large shifts in voltage-dependence (see Fig. 2). Thus, the wild type channel is only closed at negative potentials and fully open at positive potentials, while the N2E channel resides

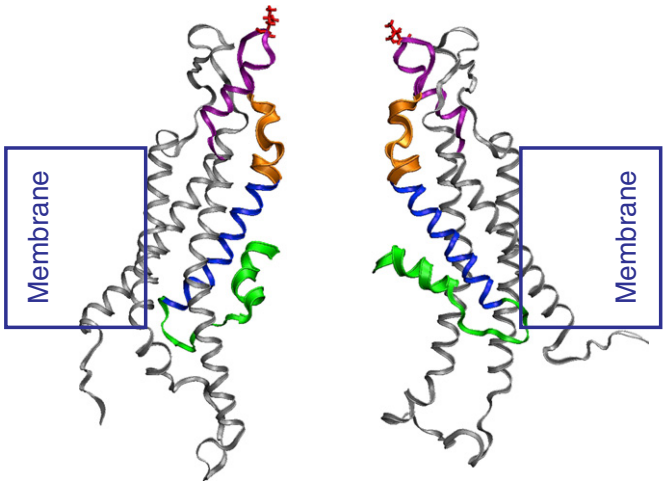

Fig. 5. Side view showing two opposite subunits of a "snapshot" the Cx26 hemichannel following equilibration by MD simulations [11]. The N-terminus is depicted by the green ribbons, with residues 1–11 shown as thick ribbons. The first transmembrane domain, TM1 is depicted by the thin blue ribbons. The 42–51 segment also termed the parahelix, which contains the 3_{10} helix described by Maeda et al. [10] is depicted by thick orange ribbons. This segment contributes to the formation of the loop-gate permeability barrier in Cx32*43E1 and Cx50 hemichannels. The first extracellular loop (E1) is depicted by the thin purple ribbons. It comprises residues 52–71. The position of the 56th residue, which demarcates the extracellular entrance to the channel pore is colored red.

in the open state at voltages around ± 20 mV, in the loop-gate closed state at voltages more negative than −20 mV and in the V_j-closed state at voltages more positive than +20 mV. Thus, comparisons of Cd^{2+} bridge formation of cysteine substitutions on wild type and N2E backgrounds allows unequivocal distinction of Cd^{2+} effects on the open, loop-gate closed and V_j-closed states (i.e. state-dependence). This contrasts the behavior of Cx26 hemichannels, where neutralization of D2 residue to reverse V_j-gating polarity (so that both V_j- and loop-gates close with hyperpolarization) is accompanied by a large inward shift in the conductance–voltage relation [68] such that open probability is ~0.5 at $V_j = 0$ mV. Cx50 hemichannels display bi-polar fast-gating, i.e. fast transitions to substates are observed at both positive and negative potentials, but the channel is fully open in the absence of membrane potential [64]. In this case, studies of conformational changes of loop-gating utilized the differential sensitivity of the Cx50 loop (slow)-gate and fast (V_j)-gate to Ca^{2+} and K^+ to distinguish the two gating mechanisms [34] and infer that Cd^{2+} formed metal bridges only with loop-gate closure.

The most significant conformational change with loop-gate closure occurs in the region of the Cx26 channel pore formed by residues 42–51, which contains a small segment termed the 3_{10} helix by Maeda et al. [10]. The structure of a snapshot of the Cx26 hemichannel following equilibration by MD simulations (Kwon et al. [11]) is presented in Fig. 5. The position of the 42–51 segment, whose structure is best described as a parahelix [93] rather than a 3_{10} helix is indicated by thick orange ribbons.

The effects of Cd^{2+}–Cys metal bridge formation and crosslinking by the homobifunctional reagent dibromobimane (bBBr) on voltage gating of two cysteine substitutions, A40C and A43C were extensively characterized in wild type and N2E backgrounds. In the Cx26 crystal structure, these residues are positioned within a hydrophobic core that includes a network of intra-subunit van der Waals interactions with residues A39, A40, V43, W44 and I74 [10]. Neither cysteine substitution was modified by MTSEA-biotin in single channel recording, indicating that they probably do not line the pore of the open 43E1 hemichannel, in agreement with the Cx26 structure. However, cysteine substitutions of two flanking residues V38 and G45 were modified when the channel resided in the open state, which indicates that these residues line the channel pore. Notably, V38 is not pore lining in the Cx26 crystal structure [10] nor does it have a high probability of pore lining in MD simulations [11]. This result can be explained by either postulating that a small difference in the structure of the open channel exists for Cx26 and 43E1, or that the cysteine substitution causes small conformation changes. Along these lines, it should be noted that the reaction of cysteine residues to MTSEA reagents requires a deprotonated, S^-, atom [94]. A charged cysteine residue is expected to prefer the aqueous environment of the channel pore in the absence of suitable countercharge within the transmembrane environment.

Application of μM concentrations of Cd^{2+} to A43C and N2E + A43C undocked hemichannels channels resulted in state-dependent lock of the channel at voltages that favored channel residency in the loop-gate closed state. Cd^{2+} had little or no effect on macroscopic conductance at inside positive voltages that favored A43C hemichannel residency in the open state and no effect on N2E + A43C channels at voltage that favor entry into a V_j-closed state. Furthermore, the kinetics

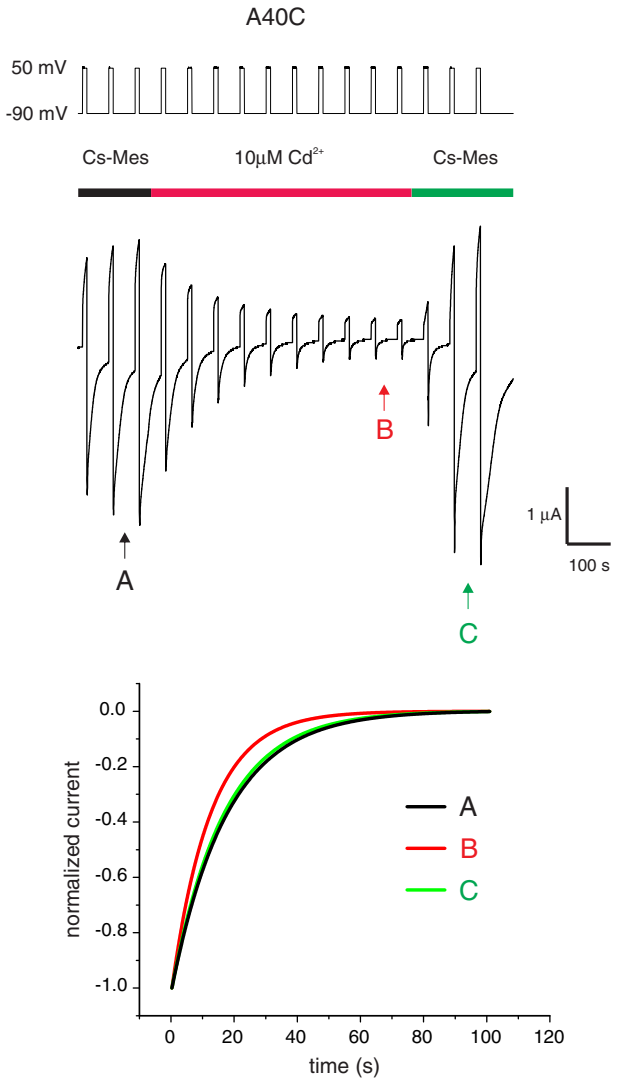

Fig. 6. Cd^{2+} lock of Cx32*43E1 A40C hemichannels is reversed by removal of Cd^{2+} by wash with bath solution. Current traces elicited by voltage steps from −90 to 50 mV are shown. The time of Cd^{2+} application is indicated by the red line. Wash with bath solution containing 100 mM cesium methanesulfonate (CsMes), 1.8 mM $CaCl_2$ and 10 mM HEPES pH 7.6 reversed Cd^{2+} lock. The increase in current at the end of the trace most likely results from the incorporation of new channels into the oocyte plasma membrane during the course of the experiment. Kinetics of channel closure before, during and after Cd^{2+} application (at A, B, and C respectively) are compared in the lower panel. The time constants of loop-gate closure are faster in the presence of Cd^{2+} as expected if Cd^{2+} stabilizes the loop-gate closed state (see text).

of channel closure became faster in the presence of Cd^{2+}. This result is consistent with the stabilization of the loop-gate closed state by Cd^{2+}, which would slow the rate of channel opening at a given voltage (Fig. 4). Application of Cd^{2+} at hyperpolarizing potentials effectively "drives" the channel into a loop-gate closed conformation. Reversal of the Cd^{2+}-lock of the loop-gate closed state could be accomplished only by application of 5–10 μM of either TPEN (N,N,N′,N′-tetrakis(2-pyridylmethyl)ethylenediamine) or DTT (dithiothreitol), known high affinity Cd^{2+} chelators. The analyses of heteromeric channels containing mixtures of wild type and A43C subunits suggested that at least four A43C subunits were required to produce high affinity Cd^{2+} binding. These results were interpreted to indicate that the high affinity binding site formed by A43C most likely resulted from the formation of a tetradentate Cd^{2+} co-ordination site. In parallel and supporting studies, 1 mM bBBr, which cross-links cysteine residues when they are separated by 3.2–6.7 Å, caused an irreversible reduction in A43C membrane currents at voltages that favor loop-gate closure.

Based on these considerations, it was proposed that at least four (but probably all) substituted cysteines at the 43rd locus moved into the 43E1 channel pore on loop-gate closure and that distance separating adjacent thiol groups of the cysteine residues was between 3.5 and 4 Å, depending on the assumption of either an octahedral or tetrahedral coordination geometry involving any four of the six subunits. This interpretation was supported by demonstration of disulfide bond formation by western blots of oocytes expressing A43C hemichannels inserted in the oocyte plasma membrane cultured in 5 mM Ca^{2+}, a condition that favors loop-gate closure. This result was interpreted to indicate that adjacent pairs of cysteine residues could approach to within ~2 Å when the channel was loop-gate closed. Because Cd^{2+} coordination is a dynamic process, leading to the adoption of the lowest free energy conformation, the ability of adjacent cysteines to approach to within 2 Å is compatible with the formation of tetradendate coordination site. However, it should be kept in mind that Ca^{2+} could induce a conformational change, as shown by AFM studies discussed above, that may be distinct from the voltage-dependent loop-gate closed state. Nonetheless, it is important to remember that the Cd^{2+} mediated stabilization of the closed loop-gate driven by voltage is not Ca^{2+} dependent. Identical Cd^{2+} lock of voltage-dependent loop-gates is observed when records are obtained in Mg^{2+} containing Ca^{2+} free bath solutions and in recording solutions containing low concentrations of divalent cations.

A40C hemichannels could also be locked in the loop-gate closed conformation with 10 μM Cd^{2+}. The reduction in current was accompanied by a faster time constant of loop-gate closure, consistent with Cd^{2+} stabilization of the loop-gate closed state (Fig. 6). However, unlike A43C, for A40C the lock in the closed state was readily reversed by wash with Cd^{2+} free solutions. The apparent lower affinity of Cd^{2+} to the cysteine site formed by A40C residues could be explained if A40C channels participate in a bidentate but not a tetradendate interaction with Cd^{2+}. This would occur if the participating cysteine residues were separated by more than the 3.5 to 4 Å required for a tetradentate interaction and coordination with a tetrahedral or octahedral geometry, but ≤5 Å, i.e. 2× the Cd—S bond length required for a less stable bidentate geometry. bBBr also caused an irreversible reduction in A40C membrane currents with hyperpolarization consistent with adjacent cysteine residues being separated by 3.2–6.7 Å in the loop-gate closed state. There was no evidence of disulfide bond formation in A40C channels indicating that the thiol groups do not approach to within 2 Å when the channel is closed, unlike for A43C channels.

Together, these results indicate that closure of the loop-gate involves position 43 in the connexin monomers coming into close proximity. They also suggest that position 40 in the connexin monomers become closer than in the open state, but not as close as position 43.

Recent unpublished results from the Bargiello lab indicate that A50C is modified by MTSEA-biotin-X when the 43E1 hemichannel resides in the open state and that it can be locked in a state-dependent manner by Cd^{2+} at inside negative voltages that favor loop-gate closure. Q56C, a substituted cysteine located at the extracellular entrance of the channel pore (Fig. 5), does not interact with Cd^{2+}, nor is gating of this mutant altered following bBBr application when it is closed by voltage. Because closure of both V_j- and loop-gates is favored at inside positive potentials, the result indicates that the extracellular entrance of the channel at Q56C does not undergo a large conformational change for either gating process.

Table 1 summarizes available SCAM, Cd^{2+}–Cys metal bridge formation and crosslinking data for cysteine mutations in the 43E1 hemichannel. Residues depicted in bold are those that interact with Cd^{2+} in the loop-gate closed conformation. Taken together these results indicate that the segment bounded by residues 43–50 undergoes a substantial conformational change with loop-gate closure. Movement of residues in the segment bounded by the 43rd to 50th

Table 1
Summary of results for substituted cysteines in the 43E1 hemichannel.

RESIDUE	Open state modified by MTSEA-biotin X	DTT/TPEN/TCEP effect on initial current	Cd^{2+} effect when channel is open	Cd^{2+} effect when loopgate closed	Dibromobimane modification when loop gate closed	Disulfide bonds in western blots
V37C	No	None	None	None	Not tested	No
V38C	Yes	None	Small decrease reversed by wash	None	Not tested	No
A39C	No	None	None	None	Not tested	No
A40C	No	None	None	Large decrease, reversed by wash	Yes	No
E41C	Low expression not tested	None	Low expression not tested	Low expression not tested	Low expression not tested	No
S42C	Low expression not tested	None	Low expression not tested	Low expression not tested	Low expression not tested	No
A43C	No	Large increase, but variable between oocytes	None	Large decrease, only reversed by DTT, TPEN, TCEP	Yes	Yes dimers formed
W44C	No expression	None	No expression	No expression	No expression	No expression
G45C	Yes	Variable	Small decrease reversed by wash	Variable effect between oocytes batches. in some cases moderate to large decrease with partial reversal by wash	Not tested	
A50C	Yes	None	Small decrease reversed by wash	Large decrease, partially reversed by wash	Not tested	Not tested
Q56C	Labeled by Alexa-Fluor 488 C5-maleimide	None	None	None	None	Not tested

Mutations that interact with Cd^{2+} are depicted in bold italics. Abbreviations: DTT—dithiothreitol; TPEN—N,N,N′,N′-tetrakis(2-pyridylmethyl)ethylenediamine; TCEP—tris(2-carboxyethyl)phosphine hydrochloride.

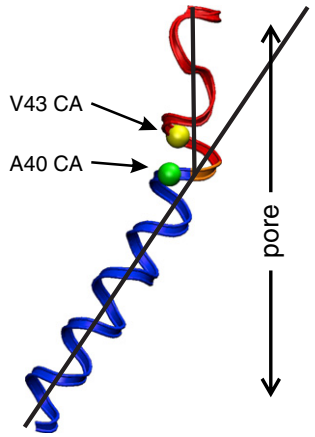

Fig. 7. Structure of the TM1/E1 bend angle in a representative Cx26 subunit following equilibration with MD simulation [11]. The positions of the Cα atoms of V43 and A40 are represented by the yellow and green spheres respectively. TM1 is depicted by the blue helix. The segment depicted in red corresponds to residues 41–50, and forms the major part of the loop-gate permeability barrier. The structure shown corresponds to the open channel conformation. In the closed conformation of Cx32*43E1, the geometry of the 41–50 segment changes such that the 43rd and 50th loci move into the channel pore. A40C in 43E1 forms a "lower affinity" Cd^{2+} binding site, which can be accomplished by straightening the bend angle. The pore diameter formed by the 41–50 segment decreases from ~15–20 to 4 Å in the loop-gate closed state.

loci reduces the channel pore from ~20 Å in the open state to ≤4 Å in the closed state. The data also indicate translocation of the 43rd residue out of the van der Waals network and into the channel pore with loop-gate closure. Notably, this change in the structure of the 42–51 segment, which we define as the parahelix is local, as D50C, which lines the pore of the open channel, also interacts with Cd^{2+} when the channel is closed by voltage, but the conformational change does not extend to cysteine substitutions of the 56th residues, which demarcates the extracellular entrance to the pore (Fig. 5). We propose that voltage destabilizes the geometry of the parahelix causing it to protrude into the channel lumen. Initially, we had proposed that loop-gate closure might involve an axial rotation of the TM1/E1 domain [56], but this seems less likely from a thermodynamic perspective, as

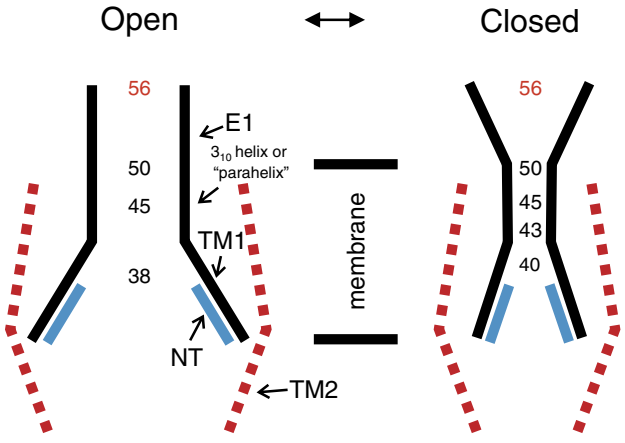

Fig. 8. Schematic representation of the open and loop-gate closed states of a connexin hemichannel, based on studies of conformational changes in the Cx32*Cx43E1 hemichannel. Residues depicted to line the pore of the open channel were determined by substituted cysteine accessibility method using MTSEA-biotin-X as the thiol modifying reagent. The pore diameter in the region of residues depicted in black in the closed model are inferred from the ability of cysteine substitutions at these loci to form metal bridges and/or to be cross-linked by bBBr. The 56th residue is depicted in red to denote that its position does not change substantially with channel closure in either V_j- or loop-gating.

such rotation would require extensive reorganization of van der Waals and electrostatic networks that stabilize the open conformation. The reversible interaction of A40C with Cd^{2+} (which is consistent with lower affinity bidentate coordination) requires that the distance among adjacent cysteine residues is somewhat larger, ~5.0 Å than those of A43C, 3.5–4 Å, predicted for high affinity tetradentate coordination. Because A40 is located in TM1 on the other side of the TM1/E1 bend where A43 is located (Fig. 7), the data suggest that the conformational change also involves straightening of the TM/E1 bend angle. This would result in narrowing of the intracellular entrance to the channel pore, but it is unlikely that this reduction would fully prevent ion flux. A schematic representation of the open and loop-gate closed state of the 43E1 hemichannel, based on current data, is presented in Fig. 8.

A somewhat different microscopic view arose from studies of metal bridge formation in undocked Cx50 hemichannels [34]. In this study, substituted cysteines of three pore lining residues F43C, G46C and D51C were shown to form Cd^{2+} binding sites under conditions that favor loop-gate closure. The affinity of Cd^{2+} binding appeared to be less at D51C than F43C, suggesting that a smaller conformational change occurs at this position. Cd^{2+} had no effect on gating of A40C and A41C Cx50 hemichannels. (Note that residue numbering of Cx50 is one more than for Cx32*43E1, e.g. A40 in 43E1 corresponds to A41 in Cx50.) Thus, there did not appear to be a local change in helical geometry, although the effect of Cd^{2+} on gating of the homologous residue Cx50 V44 (43 in 43E1) was not examined. The failure of either A40(39)C or A41(40)C to interact with Cd^{2+} also suggests a difference in the TM1/E1 bend angle in Cx50 and Cx32*43E1 hemichannels. The TM1/E1 bend angle may not straighten as much in Cx50 as it appears to do in 43E1 with loop-gate closure. It is possible that the difference in the conformation of the loop-gate closed state in the two types of hemichannels is related to difference in the organization and strength of the van der Waals networks in the two connexins due to differences in primary sequence. However it is likely that the basic loop-gating mechanism, protrusion of the parahelix (which contains the 3_{10} segment) into the channel pore, is similar if not identical in the two hemichannels.

5. Conformational changes associated with V_j-gate closure

As mentioned previously, the molecular determinants of V_j-/fast gating appear to differ among connexins. Two different mechanisms have been proposed to account for channel entry into substates: conformational changes resulting from movement of a voltage sensor located in the N-terminus as for Cx26 and Cx32 [53, 67, 69] and a particle-receptor mechanism (ball and chain model) for Cx43 and Cx40 where the CT acts as a gating particle by binding to a receptor located in the CL [37, 44, 95]. It should be noted that the original use of the term fast-gating for Cx43 was based on a component of the fast time course of current relaxations (Revilla et al. [44], not the speed of gating transitions as defined by Trexler et al. [51] and Oh et al. [69]). Subsequently, the relation of the fast kinetic component to the fast gating transition of Cx43 and Cx40 into a substate was established by single channel recordings [43, 72, 95]. A comprehensive discussion of the relation between fast and slow gating transitions, voltage dependence and kinetics of current relaxations is presented by Bukauskas and Verselis [13]. It should also be noted that to this date, no studies have demonstrated the operation of the two different fast processes in the same hemichannel. It is possible that the ball and chain mechanism is unique to some channels exemplified by Cx43 and Cx40, while conformational changes initiated by movement of the NT are unique to other channel exemplified by Cx26 and Cx32 channels. It is also possible that the two mechanisms are part of the same process, if for example the conformational change initiated by movement of the NT, exposed the receptor allowing binding of the particle to stabilize the closed state (see below).

Notably, studies of the state-dependence of the loop-gate closed conformation described in the preceding section for Cx32*43E1 and

Cx50 hemichannels suggest that conformational changes in the 42–51 segment do not occur or differ from loop-gate conformations with closure of the V_j-gate [56]. The demonstration that the gating polarity of V_j-gating initiated by movement of the NT of Cx32 channels can be reversed while maintaining the polarity of loop-gating [69] indicates that the two processes (loop and V_j-gating) differ mechanistically, but it does not rule out the possibility that conformational changes may occur in common domains, notably those that form the cytoplasmic entrance to the channel pore. Electrophysiological studies suggested that the pore diameter in the vicinity of the N-terminus of Cx32 is reduced with V_j-closure. This inference was based on the direction of current rectification of intercellular channels, when one hemichannel of the cell pair resides in a V_j-substate [68]. Based on modeling studies performed with solution of Poisson–Nernst–Plank (PNP) equations [96], it was proposed that the substate rectification of Cx32 channels resulted from narrowing the pore diameter in the closed hemichannel that accentuated the effect of positive charge in the cytoplasmic region of the pore. Similarly, in channels whose polarity was reversed by negative charge substitution in the NT, the direction of current rectification was consistent with the narrowing of pore diameter that accentuated the effect of negative charge in the V_j-closed hemichannel. This result was interpreted to indicate that the pore diameter of the channel in the vicinity of the 2nd residue narrowed with V_j closure. We stress that these data do not imply that the NT forms the constriction in Cx32 by itself. V_j-gating could result from larger conformational changes that narrow the cytoplasmic entrance (see [97] for example), consistent with the presence of a large energy barrier separating open and V_j closed states. Similar conclusions were reached in studies of Cx43 intercellular channels [98]. In this case the direction of current rectification could be explained by reduction of channel diameter that accentuated the effect of positive charge in the hemichannel closed to a substate by voltage.

5.1. Role of CT in Cx43 and Cx40 fast gating

An involvement of the CT in a mechanism of V_j/fast-gating has been reported for Cx43 and Cx40 [12, 43, 44, 95]. Studies that implicate a role for CT in are derived from the observation that deletion of the CT at residue 257 or adding tags (such as EGFP) to the CT of Cx43 correlate with the loss of a fast transition to a substate in single channel recordings, but not the slow transition from the fully open to fully closed state (i.e. loop-gating) [44, 72]. The fast voltage-gating mechanism for Cx43 and Cx40 channels invokes a "particle-receptor" (ball and chain) model, which proposes that an interaction between the CT and a region in CL termed L2 mediates the fast gating process. Fast gating of Cx43-CT truncation was reported to be restored by co-expression of Cx43-CT as a separate protein fragment [95], and abolished by addition of the L2 peptide [99] to the wild type channel. Together, these results suggest that the CT is a "freely moving" particle. This model is similar to that proposed to explain pH-gating by Delmar and colleagues [100] in that it invokes the same protein interactions of the CT and CL. It may be significant that Cx43 channels close fully in response to acidification, while to a substate in response to voltage. This suggests that the details of the molecular interactions between the particle and receptor may differ in chemical and voltage regulation of Cx43.

Specific regions of the CT and CL of Cx43 and Cx40 were shown to interact at pH 5.8 by translational diffusion analysis [37] and other biophysical methods [101, 102]. The structure of the peptides corresponding to portions of the CL and most or all the CT of Cx43 and Cx40 have been reported [102, 103]. Both appear to be largely unstructured but it has recently been reported that the CT becomes more structured when linked to TM4 [103]. Mutagenesis of the L2 region (H142E, which is near the CL-TM3 border) caused significant reduction in voltage induced occupancy of the substate [37]. Consistent with the interpretation of direct binding of CT and CL-L2 region was demonstration, by NMR, of disrupted structure of the H142E-L2 peptide. The regions of interactions between the CT and CL of Cx43 and Cx40 have been further defined biophysically [102]. Interestingly amino acid residues in the CT that interact with the L2 domain are located much closer to TM4 (in a segment bounded by 265–287 in Cx43) than to the end of the CT (I382), but it has yet to be shown that this *in vitro* interaction is the basis for the CT/CL interaction *in vivo*, either directly or indirectly through site directed mutagenesis. There is also evidence to indicate that the end of CT of Cx43 may also bind to L2, but this interaction involves fewer residues [102]. The AFM studies of Liu et al. [42] used antibodies directed against both regions of the CT and demonstrated that CT tail stretching determined with antibodies against the 252–270 segment was less than with antibodies directed against the end of the CT (residues 360–382). These results were interpreted to support the particle-receptor model of Cx43 gating, although it is seems reasonable to expect that a longer peptide segment be more "elastic" than a shorter segment if there is any secondary structure.

A major unanswered question, relevant to establishing the mechanism of reduction of current flux, is the position of L2 (the receptor) relative to the channel pore. If L2 lies within the channel pore, then the particle could block ion conductance by entering into the pore and binding the receptor (voltage-dependent block). If L2 lies outside the channel pore, then it is likely that voltage and/or pH causes a conformational change that exposes the receptor. In this case the "particle" would likely interact with the receptor to stabilize the "closed" conformation (i.e. increase the closed probability).

It is possible that L2 is located near or in the channel pore, as the cytoplasmic entry of the Cx26 channel is formed by the tip of TM2 at the junction of the CL (Fig. 5). However, it should be kept in mind that the structure of the Cx43 CL and its relation to the channel pore has not been determined [104], and in the primary sequence of Cx43, most of the L2 region is positioned in the second half of the CL, closer to TM3, which in the Cx26 structure lies at some distance from the channel pore (see [105] and Fig. 5).

Several features of the particle receptor model need further investigation. There is no simple explanation for the large energy barrier that appears to separate open and closed states in a "ball and chain" type of model. The binding of a freely mobile gating particle formed by a protein domain adopting a highly flexible extended conformation to a binding site near the cytoplasmic entrance to the pore is not expected to encounter significant energy barriers, particularly if the pore diameter of Cx43 is comparable to the large pore diameter of Cx26 hemichannel (~35–40 Å) at the intracellular entrance [10, 11]. The apparent long-time constant of current relaxation could reflect the probability that a gating particle finds its binding site, however the presence of 6 CT domains would suggest that this is not rate limiting. It has been estimated that the effective concentration of CT near the cytoplasmic entry could be as high as ~25 mM [102]. The number of CT subunits that interact with CL domain to effect entry into the substate has not been determined. It should also be kept in mind that a gating particle moving freely in the cytoplasm located at some distance from the channel pore is not expected to move in response to a voltage field, as the cytoplasm is equipotential at distances beyond a Debye length from the membrane or the protein surface (see [106]). Its movement will be largely diffusion limited if the CT is flexible and highly mobile as suggested by NMR. Also, it should be noted that the steepness of voltage-dependent block reflects the fraction of the electric field that is crossed by a gating particle of a given valence [91] when it binds its "receptor". In general terms, the voltage dependence of a blocking particle of given valence will be less steep if the binding site is close to the cytoplasmic entrance of the channel than if it lies deeper inside the channel pore. If the site of the CT/CL interaction (L2) is in the channel pore, close to the cytoplasmic entrance, then the voltage-dependence of the fast process would primarily reflect the valence (net charge) of the gating particle. This should be positive based on the polarity of fast voltage dependence.

If the receptor contained in L2 is not pore lining, then the observed voltage-dependence would most likely correspond to the voltage-dependence of a conformational change that exposes L2

allowing binding of the particle. In this case the energy barrier would primarily correspond to that of the conformational change that exposes the relevant amino acids in L2. The binding of the particle to the receptor would be independent of voltage, as there is no substantial voltage drop across the cytoplasm and it would not be expected to traverse a large energy barrier if it is freely mobile in the cytoplasm.

A similar role in fast-gating has been proposed for the CT of Cx32 [44] based on changes in closing kinetics of macroscopic conductance of Cx32 gap junctions. A Cx32-CT truncation (at residue 220) was reported to alter the kinetics of channel closure, reducing or removing a fast component of current relaxations of these gap junctions evident within the first 100 ms of a 5 s current trace. However the effects on the kinetics of Cx32 current relaxations were not large. The kinetics of the current relaxations of the remaining "slow" component of the truncation were faster than wild type and may have obscured the detection of the fast event observed in wild type channels. The operation of the proposed "ball and chain" mechanism in voltage-gating of Cx32 awaits confirmation by demonstration of loss of V_j-gating by single channel recordings of truncation mutants and knowledge of the location of the receptor relative to the channel pore.

The short length of the Cx26 CT (10 residues) and its distance from the channel pore argues against a mechanism in which it functions as a gating particle by interactions with the CL to block the channel pore. However, there is evidence suggesting that the CL and CT of Cx26 interact [105, 107], although no role for this interaction has been postulated in voltage-gating. V_j-gating of Cx26 gap junctions, like Cx32 junctions is characterized by entry into different subconductance states [68], rather than into a single substate as described for Cx43, which could be ascribed to the entry of a single Cx43 CT into the channel pore. The entry of Cx26 channels into multiple substates suggests that a long CT is not required for this aspect of gating behavior. Notably, truncations of the CT of Cx46, a connexin with long CT and CL domains, do not alter or abolish V_j (fast) gating (i.e. closure at depolarizing potentials) in macroscopic recordings of hemichannels expressed in *Xenopus* oocytes ([108] and also Kwon and Bargiello, unpublished observations). This suggests that the particle-receptor gating mechanism may not operate in all connexin channels, but additional studies are required. The central question is whether the particle acts as a "blocking" particle, or if it stabilizes a closed state, following exposure of the L2 receptor as part of a larger conformational change initiated by voltage.

5.2. Role of the N-terminus

The role of the N-terminus in determining the polarity of V_j-gating in Cx32 and Cx26 hemichannels is well established [52, 53, 67, 69] and makes clear that the N-terminus comprises at least a portion of the voltage sensor, but these studies of gating polarity do not define the conformational change associated with entry into substates. Little information derived from electrophysiological studies of V_j-gating can be used to directly inform the conformation of V_j-closed state. As mentioned previously, the rectification of currents through substates reported in Cx32 intercellular channels suggests that the intracellular entrance in the vicinity of the NT narrows with V_j-gate closure. Studies using metal-bridge formation and chemical crosslinking have the potential to define the structure of the V_j-closed state.

A role for the NT in voltage gating has been suggested in other connexins. Charge neutralization at the D3 position in Cx46 and Cx50 hemichannels appear to reverse the polarity of V_j-gating [64, 109]. The Cx50 study [109] was based on the asymmetry of the conductance–voltage relation of the heterotypic junction, Cx50/Cx50D3N, with closure observed for a single polarity of V_j, but the results need to be confirmed by single channel recording, as it has been reported that wild type Cx50 hemichannels display bi-polar fast gating events in single channel recordings [64]. Other studies have established a role of the N-terminus in gating and permeation [110–112].

The critical feature of Cx26 and Cx32 channels is the location of the NT within the channel pore, as in this position it can sense changes in V_j. It was proposed that the positioning of the Cx26 and Cx32 N-termini within the pore depends on the formation of a flexible open turn initiated by the conserved G12 residue in these group 1 or β connexins [113, 114]. This prediction is consistent with the Cx26 crystal structure. However, it should be noted that an NMR study has shown that the solution structure of a Cx37 NT peptide (a group 2 (α) connexin) differs from that of Cx32 and Cx26 in lacking a flexible open turn at the 12th position [110, 113, 114]. It is unclear how the NT of Cx37 is positioned in the channel pore. Furthermore, studies have shown that the N-terminal Met residues of Cx46 and Cx50 native hemichannels are cleaved and the penultimate glycine residue acetylated [115]. This co-translational charge modification, which neutralizes the positive charge of the N-terminal amine and the potential structural differences in the NT could play a significant role in determining both V_j-gating and ion permeation of group 2 (α) connexins. The N-terminal amine of Met1 has been shown to be acetylated in Cx26 [116], a modification that is expected to increase the electrostatic effect of the D2 residue (see Kwon et al. [11]), which has been shown to determine the gating polarity of Cx26 hemichannels [67]. Notably at least a fraction of Cx32 N-termini of Cx32 proteins are not acetylated as N-terminal sequence is obtained with the Edman degradation method [117, 118]. Acetylation blocks the N-terminus in this sequencing method. Thus, it is unclear where the positive charge required for the polarity of wild type Cx32 V_j-gating [67] is located. It may involve partial charges resulting from the dipole moment of neutral residues. Notably, all neutral and positive charge substitutions of the second Asn residue of Cx32 maintain wild type gating polarity, as do positive charge substitutions at the 5th and 8th positions [53, 67]

The studies of Oh et al. [53, 69] reveal several aspects of V_j-gating in Cx32*43E1 and N2ECx32*43E1 hemichannels that must be kept in mind when considering the mechanism of V_j-gating initiated by the NT and possible underlying conformational changes. These include:

1) The demonstration that closure of V_j-gates can result from conformational changes in individual subunits, rather than by a "concerted" mechanism in which all 6 subunits adopt the closed conformation together.
2) That the movement of a single subunit can result in channel occupancy in more than one substate. This is demonstrated by the entry of heteromeric hemichannels containing a single N2E subunit into at least 3 different substates at positive potentials. This closure can be attributed to gating initiated by the single N2E subunit. Thus, the appearance of multiple substates in the closure of the V_j gate is not necessarily a consequence of different conformations arising from the movement of multiple subunits, but rather, it strongly suggests that any one subunit can adopt different "stable" closed conformations.
3) Several 43E1 homomeric hemichannels containing charge substitutions in the N-terminus display bi-polar V_j-gating, defined as the decrease in open probability at both inside positive and negative voltages with open probability maximal at 0 mV [52, 53]. These include, T8D, N2E + G5K, N2R + G5D. The molecular basis of bi-polar channels is best explained by modeling the V_j-voltage sensor as a center open toggle switch [53]. In this model, either the inward or outward movement of the voltage sensor initiates channel closure. The voltage sensor in a bi-polar channel would cross one energy barrier for one polarity of voltage and the other barrier for the opposite polarity of voltage. Interestingly, the voltage sensitivity of bipolar channels correlates with the sign of the charge at the 2nd residue, suggesting that charges at this position may have a larger role in determining gating polarity [53]. This suggests that a larger fraction of V_j drops over the 2nd than 5th residue in the double mutations.
4) The long time constant of V_j-gating of the N2E43E1 hemichannel depicted in Fig. 2 suggests that the open and closed states are separated by a large energy barrier. Because channels are fully open at

voltages around 0 mV, the free energy of the open state is much lower than that of the V_j-closed states. This indicates that voltage acts to destabilize the structure of the open state and to stabilize the structure of the closed states.

5.3. Gating plug model of Cx26 V_j-gating

A recently proposed model of V_j-gating [10] was based on the crystal structure of Cx26 and an electron microscopy study that showed the formation of a plug in the pore of the Cx26 mutation M34A [45, 46]. The Cx26 M34A mutation forms channels in which the open probability is low at 0 mV. Thus, it is expected to adopt a closed channel state during preparation for EM imaging. The V_j-gating model proposed is also based on the high mobility of the N-terminus (indicated by the temperature factors determined for the crystal and in MD simulations of the Cx26 hemichannel [11]) and the stabilization of the position of the N-terminus in the crystal structure by 1) an inter-subunit hydrogen bond formed between the side chain of D2 and backbone amide of T5 and 2) a van der Waals interaction between W3 and M34A. It was proposed that voltage initiates V_j-gating by breaking the inter-subunit hydrogen bonds by the inward movement of the D2 residue (i.e. toward the cytoplasm). This movement would presumably lead to the destabilization of the NT leading to the loss of the W3–M34 interaction. The net result is the movement of the N-terminus to a position that would partially occlude the channel pore. Partial occlusion is required to account for the existence of sub-conductance states with V_j-gating. The movement of all six subunits would result in formation of a gating plug as predicted by the structure of the M34A. Supplementary Fig. 10 in Maeda et al. [10] depicts an outward movement of D2 (i.e. into the channel pore) in response to positive voltage, however, their text states that D2 moves inward (towards the cytoplasm) in response to positive voltage.

However, a recent study of the functional properties of Cx26M34A channels by Oshima et al. [47] led to the conclusion that the closed state of Cx26M34A differs from that induced by trans-junctional voltage. This brings into question the model of V_j-gating in which the closed state adopts the conformation of the M34A mutation. However, the strategy to determine the structure of the voltage-gated closed state(s) may be possible with mutations that are known to cause large shifts in the voltage-dependence of Cx26 and these may define the structure of the V_j-closed state.

A potential difficulty with the gating plug model is the stability of the closed state. The concern is whether the six subunits that form the gating plug could dissociate by thermal energy alone (to reopen the pore) as required by the loss of an electrical driving force when V_j is returned to 0 mV. Recall that voltage acts to stabilize the closed stated and the V_j-gates are fully open in the absence of applied potential. Although the structure of the gating plug is not known at atomic resolution it seems likely that the structure will prove to be stable owing to potential formation of extensive inter-subunit interactions of non-polar residues comprising the N-terminus.

5.4. Role of role of a proline kink motif in TM2

The model of V_j-gating based on structure–function analyses and Monte Carlo computer simulations of the behavior of a proline kink in TM2 [97] (see also [119]) runs into difficulties when considered in terms of the Cx26 crystal structure. It was proposed that the straightening of the bend angle formed at P87 (proline-kink motif) by the destabilization of a side chain backbone hydrogen bond (the TP motif) led to channel closure. However, consideration of the direction of the TM2 bend in the crystal structure indicates that a decrease in the bend angle would *increase* the diameter of the intracellular entrance of the channel pore. Thus, the simple mechanism proposed [97] should be re-evaluated in terms of the structure and dynamic interactions of the N-terminus with TM2 in the Cx26 hemichannel.

6. Molecular dynamics simulations of the Cx26 hemichannel

Elucidation of the mechanisms of voltage-gating at the atomic level requires accurate molecular models of the open and closed states. All-atom MD simulations of the crystal and "completed" Cx26 hemichannel (which includes atoms not defined in the crystal structure) in an explicit solvated POPC membrane system [11] followed by computation of ion permeation with grand canonical Brownian Dynamics GCMC/BD simulations [120–122] indicate that it is unlikely that the crystal structure is that of the biologically active open channel. Consequently, functional inferences based on the assumption that the crystal structure represents the open channel should be interpreted cautiously.

The discrepancy in computed current–voltage (I–V) relations of crystal and completed crystal structure from those observed experimentally [8, 11] is caused primarily by the small diameter of the channel pore at the tip of the NT (in the vicinity of D2). The pore diameter of the crystal structure calculated by HOLE [123] is ~10 Å, rather than 14 Å reported by Maeda et al. [10]. The difference in the two measurements of pore diameter reflects the consideration of the atom diameters and inclusion of H atoms in measurement with HOLE, rather than measurement of minimal center-to-center distances of opposed heavy atoms. Inclusion of Met1 that was not defined in the crystal structure further exacerbates the deviation between computed and experimental data. The pore diameter is reduced to at least ~5.5 Å when Met1 is included in the structural model of Cx26 and the positive charge of the N-terminal amine of Met1 introduced a substantial barrier to cation flux, which resulted in near perfect anion selectivity and marked inward rectification of currents in GCMC/BD simulation. The increase in pore diameter, to 12.8 Å at the tip of the NT, in the "average equilibrated structure" resulted from several factors including the relaxation in the packing of all four transmembrane helices of each connexin monomer, a small change in the tilt angle of all transmembrane helices, and breakage of the inter-subunit D2—T5 hydrogen bond. This H-bond, which is proposed to stabilize the pore in the crystal structure, was broken within the first 5 ns of the equilibration stage MD simulation (140 ns) and did not reform for the duration of the production stage simulations (four replicate 20 ns simulations). The MD simulations also optimized the positions of the side chains of numerous amino acids located within the interfaces of the four transmembrane domains (see the interaction lists provided in the Supplemental Information in Kwon et al. [11]). The calculated I–V relation of the "average equilibrated structure" obtained with MD, closely matched experimental data when charge modifying co- and post-translation modifications, including N-terminal acetylation of Met1 and acetylation of several internal lysine residues, identified by the MS studies of Locke et al. [116] were taken into account. Incorporation of the same charge modifications into the crystal and completed crystal structure did not resolve deviations of computed from experimentally determined current–voltage relations. These results strongly suggest that the "average equilibrated structure" more closely represents that of the open Cx26 hemichannel than do the crystal and completed crystal structures and that protein modification plays an important role in channel permeability and voltage dependence.

Notably, the MD simulations indicated that the region of the open channel pore formed by the 40–50 segment (which contains the parahelix) is the most stable region of the Cx26 channel pore. This region, which undergoes large changes in conformation with loop-gating is stabilized by an extensive network of intra-subunit van der Waals and inter- and intra-subunit electrostatic interactions that differ somewhat from those predicted by the crystal structure. The interaction energies calculated from MD simulations are consistent with a large energy barrier separating open and closed states and suggest that the conformational changes proceed by the sequential destabilization of electrostatic and van der Waals interactions.

7. Perspective and future directions

The basic scientific question addressed by the studies presented in this review is to elucidate at the atomic level the mechanisms of voltage-dependent gating of connexin channels. The extent of the conformational change resulting from loop-gate closure is remarkable; the diameter of the most stable region of the channel pore is reduced from ~15–20 Å to ~4 Å. The stability of the segment suggests that a large energy barrier must be crossed in order to constrict the pore, change the geometry of the parahelix, and possibly straighten the TM1/E1 bend angle. The potential scale of the problem is illustrated by considering that the energy provided by a 100 mV polarization to move any given charged residue is ~3.2 kcal/mol, roughly the energy of a hydrogen bond; and one expects that a large conformational change would involve breaking and reformation of new interactions equivalent to at least several H-bonds. In addition the presence of a large van der Waals network, which stabilizes the open structure, further suggests that the energy barrier separating the open and closed states is large, although the interaction energy of individual pairs of interacting residues may be small, in the order of 1–3 kcal/mol. The central question is to determine how the large conformational change identified experimentally for loop-gating is accomplished within thermodynamic constraints.

Current studies defining the atomic structure of the open and closed states are beginning to provide the necessary framework to define the path of the molecular transitions that links the open and loop-gate closed two states. The cornerstone of these studies is the recent publication of the X-ray crystal structure of the Cx26 gap junction by Maeda et al. [10] and its refinement by MD simulations [11]. Exploring the path of molecular transitions requires accurate models of both the open and closed states.

Several computational methods are available to determine how closely a structural model corresponds to the open state. These include the GCMC/BD algorithm developed by Roux and co-workers [122, 124]. This approach is powerful but only characterizes ionic permeation through a fixed rigid structure with several approximations including implicit solvent based protein–ion interactions and an implicit membrane (see [122] and [11] for discussion). The alternative is the calculation of ion flux with MD simulations, but this method is computationally expensive and requires either very long simulations or the use of high concentrations of permeant ions and is limited to consideration of symmetric ion concentrations. The application of the two approaches is exemplified by the recent studies of Im and co-workers to evaluate different structural models of VDAC channels [122, 125]. Significantly, there was good agreement between the results obtained with GCMC/BD and MD simulations. This indicates that GCMC/BD simulations can be used to accurately predict ion flux through large pore channels. Note however that GCMC/BD simulations are not expected to provide accurate representations of ion flux through narrow, single file ion channels such as K^+ and gramicidin where the dynamics of backbone carbonyls of the selectivity filter (K^+ channels) and side chain dynamics (gramicidin) play a critical role [126, 127]. Recently, Kwon et al. [11] have applied GCMC/BD simulations to Cx26 hemichannels. The results obtained strongly suggest that the crystal structure does not represent the structure of the open channel, while the "average equilibrated structure" resulting from all atom MD simulations is likely to closely correspond more closely to the open state. The study also points to a critical role of co- and post-translational modifications, as reported by Locke et al. [116] in determining Cx26 function.

The value of MD simulations is that they not only provide a means of structural refinement but also allow quantification of the strengths and dynamics of amino acid interactions [128]. This is of particular interest as voltage acts to close connexin channels by destabilizing (i.e. increasing the free energy) the open state. In addition to the study performed by Kwon et al., an MD simulation of Cx26 hemichannel has been performed by Hung and Yarovsky [129] that identified lipid protein-interactions that may be important in stabilizing the open state. Interestingly, Cx46 and C50 hemichannels are reported to display bipolar mechanosensitivity, such that membrane distortion at hyperpolarizing potentials, which favor loop-gate closure, result in channel opening, while membrane distortion at depolarizing potentials, which favor V_j-gate closure, result in channel closure [130]. MD simulations of mechanosensitive channels have a provided a conceptual framework to explore conformational changes in response to membrane tension [131].

A critical step in understanding voltage-gating of connexin channels is to identify the structure(s) of the closed states. As discussed above, there are two experimental approaches to accomplish this goal, mutagenesis combined with electrophysiology and structural. The former, includes the use of substituted cysteines to form Cd^{2+} metal bridges and/or sites for chemical crosslinking. In essence, this approach uses metal bridge formation and chemical cross-linkers as molecular rulers to define the proximity of substituted cysteines when the channel resides in the open and closed states. Although powerful, the approach has several limitations. It relies on the creation of cysteine mutations that may alter the structure of the channel or the gating mechanism. This potential problem can be overcome by characterization of multiple sites of substituted cysteines in the same as well as different connexins. Differences among channels formed by different connexins may identify subtle differences in structure or in interactions that stabilize the open state, as may be the case for Cx32*43E1 and Cx50 hemichannels. One must also keep in mind that the interaction of Cd^{2+} with cysteines will drive the conformation of the binding site into its lowest energy conformation, raising the possibility that the Cd^{2+} bound closed conformation may differ somewhat from the "true" closed state. The proximity relations of substituted cysteines can provide constraints in the production of an atomistic model of the closed state. This strategy is illustrated by application of the ROSETTA membrane method by Yarov-Yarovoy et al. [132] and Pathak et al. [82] to model the open and resting states of the potassium channel voltage sensor. Notably, the total gating charge determined by computational calculations of these modeled structures is in good agreement with that experimentally determined for the *Shaker* potassium channel [133]. This result supports the view that the computational models derived from experimental data are a realistic depiction of the open and closed states of *Shaker* type K^+ channels, and provides confidence that similar approaches will succeed in modeling the closed state of connexin channels.

A second approach is to solve the crystal structure of mutant forms of Cx26 that favor occupancy in a particular closed state. This was the approach used by Oshima et al. [47] in their attempt to define the closed state of Cx26 by solving the structure of the Cx26 M34A channel. However, as indicated by their most recent publication [47], the approach requires careful biophysical characterizations of mutant channels to ensure that the mutation does in fact adopt a closed state corresponding to the structure of the channel closed by the intended parameter (voltage in this case). This did not appear to be the case for this mutation. The challenge faced by future structural studies is to find mutations in which the crystalized state is identical to a functional closed state. One should also keep in mind that a crystal structure represents the lowest free energy structure of the protein that produces high quality diffracting crystals. The relation of the solved crystal structure to the structure closed by voltage must be verified experimentally.

These considerations indicate that the mutagenic/electrophysiological experimental and structural approaches are synergistic with each other, and with computational approaches. Coordinated and integrated application of these methods should ultimately lead to the identification of the closed state(s) of connexin channels. In turn, this will form the basis for understanding the dynamics of a connexin channel, regarding both gating and permeation.

The ultimate goal is to define the path of the transitions linking open and closed states. The recent development of a specialized computer, Anton, has greatly expanded the time scale of MD simulations that can be performed in a reasonable period of time; from hundreds of nanoseconds, typical of most current MD simulations to

milliseconds at least for small molecular systems [134, 135]. Computers such as Anton potentially allow the application of "brute force" MD simulations to explore the conformational changes in channel structure induced by voltage. The fundamental question is how long a simulation is needed to simulate a voltage-dependent transition. There is no *a priori* answer to this question. In essence the brute force method, if conformational changes are observed, enables one to address a fundamental biophysical question; the molecular basis for the latency of channel closure in response to voltage as opposed to the actual gating event. Alternatively, other computational methods including targeted and steered molecular dynamics are available that can identify a probable transition pathway, whose energetics can be explored more fully by multiple MD simulations of structures identified along the path (see for example [131, 136]). Computational methods are being developed to map the transition path from one molecular conformation to another. A promising development is the string method with swarms of MD trajectories [137]. The development of such methods coupled with increases in computational speed and power should provide detailed atomic models of voltage-gating transitions of ion channels in the near future.

It should be noted that MD simulations are not without limitations; stemming in part from the accuracy of available force-fields (which are also "models" and require validation, see for example [126]) and the length of simulations [138]. The power of the approach to solve biological problems is derived from the ability to merge computational and experimental strategies. For example, experimental methods have been developed, notably rate-equilibrium linear free energy relationship analysis, to explore the transition state linking two stable conformations of the nicotinic acetylcholine receptor [139–141]. The method should be applicable to other ion channels and provides a means of testing the predictions of computationally derived transition paths.

Acknowledgements

This work was supported by NIH grant R01GM46889 to TAB. Additional support was provided by the Albert Einstein College of Medicine. Computational resources were provided by the Division of High Performance and Research Computing at UMDNJ and by the National Science Foundation through TeraGrid resources provided by NCSA under grant number TG-IBN090012 and by the HPC Core Service at Albert Einstein College of Medicine. We are grateful to Drs. Andrew Harris and Benoit Roux and their laboratories for discussion and insights.

References

[1] D.W. Laird, Life cycle of connexins in health and disease, Biochem. J. 394 (2006) 527–543.
[2] G. Mese, V. Valiunas, P.R. Brink, T.W. White, Connexin26 deafness associated mutations show altered permeability to large cationic molecules, Am. J. Physiol. Cell Physiol. 295 (2008) C966–C974.
[3] M.V.L. Bennett, J.E. Contreras, F.F. Bukauskas, J.C. Sáez, New roles for astrocytes: Gap junction hemichannels have something to communicate, Trends Neurosci. 26 (2003) 610–617.
[4] J.C. Saez, M.A. Retamal, D. Basilio, F.F. Bukauskas, M.V. Bennett, Connexin-based gap junction hemichannels: gating mechanisms, Biochim. Biophys. Acta 1711 (2005) 215–224.
[5] N. Palacios-Prado, S. Sonntag, V.A. Skeberdis, K. Willecke, F.F. Bukauskas, Gating, permselectivity and pH-dependent modulation of channels formed by connexin57, a major connexin of horizontal cells in the mouse retina, J. Physiol. 587 (2009) 3251–3269.
[6] L. Ebihara, J.-J. Tong, B. Vertel, T.W. White, T.-L. Chen, Properties of connexin 46 hemichannels in dissociated lens fiber cells, Investig. Ophthalmol. Vis. Sci. 52 (2011) 882–889.
[7] J.R. Lee, A.M. Derosa, T.W. White, Connexin mutations causing skin disease and deafness increase hemichannel activity and cell death when expressed in *Xenopus* oocytes, J. Invest. Dermatol. 129 (2009) 870–878.
[8] H.A. Sanchez, G. Mese, M. Srinivas, T.W. White, V.K. Verselis, Differentially altered Ca2+ regulation and Ca2+ permeability in Cx26 hemichannels formed by the A40V and G45E mutations that cause keratitis ichthyosis deafness syndrome, J. Gen. Physiol. 136 (2010) 47–62.
[9] A. Terrinoni, A. Codispoti, V. Serra, B. Didona, E. Bruno, R. Nisticò, M. Giustizieri, M. Alessandrini, E. Campione, G. Melino, Connexin 26 (GJB2) mutations, causing KID syndrome, are associated with cell death due to calcium gating deregulation, Biochem. Biophys. Res. Commun. 394 (2010) 909–914.
[10] S. Maeda, S. Nakagawa, M. Suga, E. Yamashita, A. Oshima, Y. Fujiyoshi, T. Tsukihara, Structure of the connexin 26 gap junction channel at 3.5 A resolution, Nature 458 (2009) 597–602.
[11] T. Kwon, A.L. Harris, A. Rossi, T.A. Bargiello, Molecular dynamics simulations of the Cx26 hemichannel: evaluation of structural models with Brownian dynamics., Journal of General Physiology, in press (2011).
[12] D. González, J.M. Gómez-Hernández, L.C. Barrio, Molecular basis of voltage dependence of connexin channels: an integrative appraisal, Progress in Biophysics and Molecular Biology 94 (2007) 66–106.
[13] F.F. Bukauskas, V.K. Verselis, Gap junction channel gating, Biochimica et Biophysica Acta (BBA) Biomembranes 1662 (2004) 42–60.
[14] T. Bargiello, P. Brink, Voltage-gating mechanisms of connexin channels, in: A.L. Harris, D. Locke (Eds.), Connexins, Humana Press, 2009, pp. 103–128.
[15] S. Oh, Y. Ri, M.V. Bennett, E.B. Trexler, V.K. Verselis, T.A. Bargiello, Changes in permeability caused by connexin 32 mutations underlie X-linked Charcot–Marie–Tooth disease, Neuron 19 (1997) 927–938.
[16] X.Q. Gong, B.J. Nicholson, Size selectivity between gap junction channels composed of different connexins, Cell Commun. Adhes. 8 (2001) 187–192.
[17] E.R. Nightingale, Phenomenological theory of ion solvation. Effective radii of hydrated ions, J. Phys. Chem. 63 (1959) 1381–1387.
[18] H. Eyring, The activated complex and the absolute rate of chemical reactions, Chem. Rev. 17 (1935) 65–77.
[19] P.N. Unwin, P.D. Ennis, Calcium-mediated changes in gap junction structure: evidence from the low angle X-ray pattern, J. Cell Biol. 97 (1983) 1459–1466.
[20] P.N. Unwin, P.D. Ennis, Two configurations of a channel-forming membrane protein, Nature 307 (1984) 609–613.
[21] P.N.T. Unwin, G. Zampighi, Structure of the junction between communicating cells, Nature 283 (1980) 545–549.
[22] M.V. Bennett, L.C. Barrio, T.A. Bargiello, D.C. Spray, E. Hertzberg, J.C. Saez, Gap junctions: new tools, new answers, new questions, Neuron 6 (1991) 305–320.
[23] D.J. Muller, G.M. Hand, A. Engel, G.E. Sosinsky, Conformational changes in surface structures of isolated connexin 26 gap junctions, EMBO J. 21 (2002) 3598–3607.
[24] G.E. Sosinsky, B.J. Nicholson, Structural organization of gap junction channels, Biochim. Biophys. Acta 1711 (2005) 99–125.
[25] M.J. Allen, J. Gemel, E.C. Beyer, R. Lal, Atomic force microscopy of Connexin40 hemichannels reveals calcium-dependent 3D molecular topography and open-closed conformations of both the extracellular and cytoplasmic faces, J. Biol. Chem. 286 (2011) 22139–22146.
[26] C. Newton, W. Pangborn, S. Nir, D. Papahadjopoulos, Specificity of Ca2+ and Mg2+ binding to phosphatidylserine vesicles and resultant phase changes of bilayer membrane structure, Biochimica et Biophysica Acta (BBA) Biomembranes 506 (1978) 281–287.
[27] H. Träuble, H. Eibl, Electrostatic effects on lipid phase transitions: membrane structure and ionic environment, Proc. Natl. Acad. Sci. 71 (1974) 214–219.
[28] R.S. Vest, L.J. Gonzales, S.A. Permann, E. Spencer, L.D. Hansen, A.M. Judd, J.D. Bell, Divalent cations increase lipid order in erythrocytes and susceptibility to secretory phospholipase A2, Biophys. J. 86 (2004) 2251–2260.
[29] V.K. Verselis, M. Srinivas, Divalent cations regulate connexin hemichannels by modulating intrinsic voltage-dependent gating, J. Gen. Physiol. 132 (2008) 315–327.
[30] J.M. Gómez-Hernández, M. de Miguel, B. Larrosa, D. González, L.C. Barrio, Molecular basis of calcium regulation in connexin-32 hemichannels, Proc. Natl. Acad. Sci. 100 (2003) 16030–16035.
[31] M.C. Puljung, V.M. Berthoud, E.C. Beyer, D.A. Hanck, Polyvalent cations constitute the voltage gating particle in human connexin37 hemichannels, J. Gen. Physiol. 124 (2004) 587–603.
[32] H. Ripps, H. Qian, J. Zakevicius, Properties of connexin26 hemichannels expressed in *Xenopus* oocytes, Cell. Mol. Neurobiol. 24 (2004) 647–665.
[33] L. Ebihara, X. Liu, J.D. Pal, Effect of external magnesium and calcium on human connexin46 hemichannels, Biophys. J. 84 (2003) 277–286.
[34] V.K. Verselis, M.P. Trelles, C. Rubinos, T.A. Bargiello, M. Srinivas, Loop gating of connexin hemichannels involves movement of pore-lining residues in the first extracellular loop domain, J. Biol. Chem. 284 (2009) 4484–4493.
[35] A.K. Katz, J.P. Glusker, S.A. Beebe, C.W. Bock, Calcium ion coordination: a comparison with that of beryllium, magnesium, and zinc, J. Am. Chem. Soc. 118 (1996) 5752–5763.
[36] S. Liu, S. Taffet, L. Stoner, M. Delmar, M.L. Vallano, J. Jalife, A structural basis for the unequal sensitivity of the major cardiac and liver gap junctions to intracellular acidification: the carboxyl tail length, Biophys. J. 64 (1993) 1422–1433.
[37] J. Shibayama, C. Gutierrez, D. Gonzalez, F. Kieken, A. Seki, J.R. Carrion, P.L. Sorgen, S.M. Taffet, L.C. Barrio, M. Delmar, Effect of charge substitutions at residue his-142 on voltage gating of connexin43 channels, Biophys. J. 91 (2006) 4054–4063.
[38] J. Shibayama, R. Lewandowski, F. Kieken, W. Coombs, S. Shah, P.L. Sorgen, S.M. Taffet, M. Delmar, Identification of a novel peptide that interferes with the chemical regulation of connexin43, Circ. Res. 98 (2006) 1365–1372.
[39] B.J. Hirst-Jensen, P. Sahoo, F. Kieken, M. Delmar, P.L. Sorgen, Characterization of the pH-dependent interaction between the gap junction protein connexin43 carboxyl terminus and cytoplasmic loop domains, J. Biol. Chem. 282 (2007) 5801–5813.
[40] R. Lewandowski, J. Shibayama, E.M. Oxford, R. Joshi-Mukherjee, W. Coombs, P.L. Sorgen, S.M. Taffet, M. Delmar, Chemical gating of connexin channels, in: A.L. Harris, D. Locke (Eds.), Connexins, Humana Press, 2009, pp. 129–142.
[41] E. Brady Trexler, F.F. Bukauskas, M.V.L. Bennett, T.A. Bargiello, V.K. Verselis, Rapid and direct effects of pH on connexins revealed by the connexin46 hemichannel preparation, J. Gen. Physiol. 113 (1999) 721–742.

[42] F. Liu, F.T. Arce, S. Ramachandran, R. Lal, Nanomechanics of hemichannel conformations, J. Biol. Chem. 281 (2006) 23207–23217.
[43] J.M.B. Anumonwo, S.M. Taffet, H. Gu, M. Chanson, A.P. Moreno, M. Delmar, The carboxyl terminal domain regulates the unitary conductance and voltage dependence of connexin40 gap junction channels, Circ. Res. 88 (2001) 666–673.
[44] A. Revilla, C. Castro, L.C. Barrio, Molecular dissection of transjunctional voltage dependence in the connexin-32 and connexin-43 junctions, Biophys. J. 77 (1999) 1374–1383.
[45] A. Oshima, K. Tani, Y. Hiroaki, Y. Fujiyoshi, G.E. Sosinsky, Three-dimensional structure of a human connexin26 gap junction channel reveals a plug in the vestibule, Proc. Natl. Acad. Sci. 104 (2007) 10034–10039.
[46] A. Oshima, K. Tani, Y. Hiroaki, Y. Fujiyoshi, G.E. Sosinsky, Projection structure of a N-Terminal deletion mutant of connexin 26 channel with decreased central pore density, Cell Commun. Adhes. 15 (2008) 85–93.
[47] A. Oshima, K. Tani, M.M. Toloue, Y. Hiroaki, A. Smock, S. Inukai, A. Cone, B.J. Nicholson, G.E. Sosinsky, Y. Fujiyoshi, Asymmetric configurations and N-terminal rearrangements in connexin26 gap junction channels, J. Mol. Biol. 405 (2011) 724–735.
[48] V.K. Verselis, M.V. Bennett, T.A. Bargiello, A voltage-dependent gap junction in *Drosophila melanogaster*, Biophys. J. 59 (1991) 114–126.
[49] A.L. Harris, D.C. Spray, M.V. Bennett, Kinetic properties of a voltage-dependent junctional conductance, J. Gen. Physiol. 77 (1981) 95–117.
[50] D.L. Paul, L. Ebihara, L.J. Takemoto, K.I. Swenson, D.A. Goodenough, Connexin46, a novel lens gap junction protein, induces voltage-gated currents in nonjunctional plasma membrane of *Xenopus* oocytes, J. Cell Biol. 115 (1991) 1077–1089.
[51] E.B. Trexler, M.V. Bennett, T.A. Bargiello, V.K. Verselis, Voltage gating and permeation in a gap junction hemichannel, Proc. Natl. Acad. Sci. 93 (1996) 5836–5841.
[52] P.E.M. Purnick, S. Oh, C.K. Abrams, V.K. Verselis, T.A. Bargiello, Reversal of the gating polarity of gap junctions by negative charge substitutions in the N-terminus of connexin 32, Biophys. J. 79 (2000) 2403–2415.
[53] S. Oh, S. Rivkin, Q. Tang, V.K. Verselis, T.A. Bargiello, Determinants of gating polarity of a connexin 32 hemichannel, Biophys. J. 87 (2004) 912–928.
[54] S. Oh, V.K. Verselis, T.A. Bargiello, Charges dispersed over the permeation pathway determine the charge selectivity and conductance of a Cx32 chimeric hemichannel, J. Physiol. 586 (2008) 2445–2461.
[55] A. Pfahnl, G. Dahl, Localization of a voltage gate in connexin46 Gap junction hemichannels, Biophys. J. 75 (1998) 2323–2331.
[56] Q. Tang, T.L. Dowd, V.K. Verselis, T.A. Bargiello, Conformational changes in a pore-forming region underlie voltage-dependent "loop gating" of an unapposed connexin hemichannel, J. Gen. Physiol. 133 (2009) 555–570.
[57] E.B. Trexler, F.F. Bukauskas, J. Kronengold, T.A. Bargiello, V.K. Verselis, The first extracellular loop domain is a major determinant of charge selectivity in connexin46 channels, Biophys. J. 79 (2000) 3036–3051.
[58] X.W. Zhou, A. Pfahnl, R. Werner, A. Hudder, A. Llanes, A. Luebke, G. Dahl, Identification of a pore lining segment in gap junction hemichannels, Biophys. J. 72 (1997) 1946–1953.
[59] J. Kronengold, E.B. Trexler, F.F. Bukauskas, T.A. Bargiello, V.K. Verselis, Single-channel SCAM identifies pore-lining residues in the first extracellular loop and first transmembrane domains of Cx46 hemichannels, J. Gen. Physiol. 122 (2003) 389–405.
[60] M.H. Akabas, D.A. Stauffer, M. Xu, A. Karlin, Acetylcholine receptor channel structure probed in cysteine-substitution mutants, Science 258 (1992) 307–310.
[61] I.M. Skerrett, J. Aronowitz, J.H. Shin, G. Cymes, E. Kasperek, F.L. Cao, B.J. Nicholson, Identification of amino acid residues lining the pore of a gap junction channel, J. Cell Biol. 159 (2002) 349–360.
[62] N. Paulauskas, M. Pranevicius, H. Pranevicius, F.F. Bukauskas, A stochastic four-state model of contingent gating of gap junction channels containing two "fast" gates sensitive to transjunctional voltage, Biophys. J. 96 (2009) 3936–3948.
[63] R. Vogel, R. Weingart, Mathematical model of vertebrate gap junctions derived from electrical measurements on homotypic and heterotypic channels, J. Physiol. 510 (1998) 177–189.
[64] M. Srinivas, J. Kronengold, F.F. Bukauskas, T.A. Bargiello, V.K. Verselis, Correlative studies of gating in Cx46 and Cx50 hemichannels and gap junction channels, Biophys. J. 88 (2005) 1725–1739.
[65] L. Ebihara, V.M. Berthoud, E.C. Beyer, Distinct behavior of connexin56 and connexin46 gap junctional channels can be predicted from the behavior of their hemi-gap-junctional channels, Biophys. J. 68 (1995) 1796–1803.
[66] D.L. Beahm, J.E. Hall, Hemichannel and junctional properties of connexin 50, Biophys. J. 82 (2002) 2016–2031.
[67] V.K. Verselis, C.S. Ginter, T.A. Bargiello, Opposite voltage gating polarities of two closely related onnexins, Nature 368 (1994) 348–351.
[68] S. Oh, J.B. Rubin, M.V. Bennett, V.K. Verselis, T.A. Bargiello, Molecular determinants of electrical rectification of single channel conductance in gap junctions formed by connexins 26 and 32, J. Gen. Physiol. 114 (1999) 339–364.
[69] S. Oh, C.K. Abrams, V.K. Verselis, T.A. Bargiello, Stoichiometry of transjunctional voltage-gating polarity reversal by a negative charge substitution in the amino terminus of a connexin32 chimera, J. Gen. Physiol. 116 (2000) 13–31.
[70] F.F. Bukauskas, R. Weingart, Voltage-dependent gating of single gap junction channels in an insect cell line, Biophys. J. 67 (1994) 613–625.
[71] A. Pfahnl, X.W. Zhou, R. Werner, G. Dahl, A chimeric connexin forming gap junction hemichannels, Pflugers Archiv Eur. J. Physiol. 433 (1997) 773–779.
[72] F.F. Bukauskas, A. Bukauskiene, V.K. Verselis, M.V.L. Bennett, Coupling asymmetry of heterotypic connexin 45/connexin 43-EGFP gap junctions: properties of fast and slow gating mechanisms, Proc. Natl. Acad. Sci. 99 (2002) 7113–7118.
[73] M. Rackauskas, M.M. Kreuzberg, M. Pranevicius, K. Willecke, V.K. Verselis, F.F. Bukauskas, Gating properties of heterotypic gap junction channels formed of connexins 40, 43, and 45, Biophys. J. 92 (2007) 1952–1965.
[74] A.P. Moreno, J.G. Laing, E.C. Beyer, D.C. Spray, Properties of gap junction channels formed of connexin 45 endogenously expressed in human hepatoma (SKHep1) cells, Am. J. Physiol. Cell Physiol. 268 (1995) C356–C365.
[75] T. Desplantez, I. Marics, T. Jarry-Guichard, R. Veteikis, J. Briand, R. Weingart, D. Gros, Characterization of zebrafish Cx43.4 connexin and its channels, Exp. Physiol. 88 (2003) 681–690.
[76] Q.V. Hoang, H. Qian, H. Ripps, Functional analysis of hemichannels and gap-junctional channels formed by connexins 43 and 46, Mol. Vis. 16 (2010) 1343–1352.
[77] B.M. Rodríguez, D. Sigg, F. Bezanilla, Voltage gating of Shaker K+ channels, J. Gen. Physiol. 112 (1998) 223–242.
[78] D.G. Gagnon, F. Bezanilla, The contribution of individual subunits to the coupling of the voltage sensor to pore opening in Shaker K channels: effect of ILT mutations in heterotetramers, J. Gen. Physiol. 136 (2010) 555–568.
[79] A.M. Correa, F. Bezanilla, R. Latorre, Gating kinetics of batrachotoxin-modified Na+ channels in the squid giant axon. Voltage and temperature effects, Biophys. J. 61 (1992) 1332–1352.
[80] F. Bezanilla, The voltage sensor in voltage-dependent ion channels, Physiol. Rev. 80 (2000) 555–592.
[81] F. Bezanilla, Ion channels: from conductance to structure, Neuron 60 (2008) 456–468.
[82] M.M. Pathak, V. Yarov-Yarovoy, G. Agarwal, B. Roux, P. Barth, S. Kohout, F. Tombola, E.Y. Isacoff, Closing in on the resting state of the Shaker K+ channel, Neuron 56 (2007) 124–140.
[83] G. Loussouarn, L.R. Phillips, R. Masia, T. Rose, C.G. Nichols, Flexibility of the Kir6.2 inward rectifier K+ channel pore, Proc. Natl. Acad. Sci. 98 (2001) 4227–4232.
[84] J. Horenstein, P. Riegelhaupt, M.H. Akabas, Differential protein mobility of the γ-aminobutyric acid, type A, receptor α and β subunit channel-lining segments, J. Biol. Chem. 280 (2005) 1573–1581.
[85] G. Yellen, The moving parts of voltage-gated ion channels, Q. Rev. Biophys. 31 (1998) 239–295.
[86] G. Berthon, The stability constants of metal complexes of amino acids with polar side chains, Pure Appl. Chem. 67 (1995) 1117–1240.
[87] T. Vilariño, I. Brandariz, S. Fiol, J. López Fonseca, M. Sastre De Vicente, Complexation of Cd2+ by cysteine at ionic strength of 0.7 m studied by differential pulse polarography, Bull. Soc. Chim. Belg. 102 (1993) 699–707.
[88] I. Dokmanic, M. Sikic, S. Tomic, Metals in proteins: correlation between the metal-ion type, coordination number and the amino-acid residues involved in the coordination, Acta Crystallogr. D: Biol. Crystallogr. D64 (2007) 257–263.
[89] L. Rulísek, J. Vondrásek, Coordination geometries of selected transition metal ions (Co2+, Ni2+, Cu2+, Zn2+, Cd2+, and Hg2+) in metalloproteins, J. Inorg. Biochem. 71 (1998) 115–127.
[90] F. Jalilehvand, V. Mah, B.O. Leung, J.n. Mink, G.M. Bernard, L.s. Hajba, Cadmium(II) cysteine complexes in the solid state: a multispectroscopic study, Inorg. Chem. 48 (2009) 4219–4230.
[91] A.M. Woodhull, Ionic blockage of sodium channels in nerve, J. Gen. Physiol. 61 (1973) 687–708.
[92] R.J. French, J.B. Wells, Sodium ions as blocking agents and charge carriers in the potassium channel of the squid giant axon, J. Gen. Physiol. 70 (1977) 707–724.
[93] P. Enkhbayar, K. Hikichi, M. Osaki, R.H. Kretsinger, N. Matsushima, 310-helices in proteins are parahelices, Proteins Struct. Funct. Bioinf. 64 (2006) 691–699.
[94] A. Karlin, M.H. Akabas, Substituted-cysteine accessibility method, in: P.M. Conn (Ed.), Methods in Enzymology, Volume 293, Academic Press, 1998, pp. 123–145.
[95] A.P. Moreno, M. Chanson, J. Anumonwo, I. Scerri, H. Gu, S.M. Taffet, M. Delmar, Role of the carboxyl terminal of connexin43 in transjunctional fast voltage gating, Circ. Res. 90 (2002) 450–457.
[96] D. Chen, R. Eisenberg, Charges, currents, and potentials in ionic channels of one conformation, Biophys. J. 64 (1993) 1405–1421.
[97] Y. Ri, J.A. Ballesteros, C.K. Abrams, S. Oh, V.K. Verselis, H. Weinstein, T.A. Bargiello, The role of a conserved proline residue in mediating conformational changes associated with voltage gating of Cx32 gap junctions, Biophys. J. 76 (1999) 2887–2898.
[98] F.F. Bukauskas, A. Bukauskiene, V.K. Verselis, Conductance and permeability of the residual state of connexin43 gap junction channels, J. Gen. Physiol. 119 (2002) 171–186.
[99] A. Seki, H.S. Duffy, W. Coombs, D.C. Spray, S.M. Taffet, M. Delmar, Modifications in the biophysical properties of connexin43 channels by a peptide of the cytoplasmic loop region, Circ. Res. 95 (2004) e22–e28.
[100] J.F. Ek-Vitorín, G. Calero, G.E. Morley, W. Coombs, S.M. Taffet, M. Delmar, pH regulation of connexin43: molecular analysis of the gating particle, Biophys. J. 71 (1996) 1273–1284.
[101] M. Delmar, W. Coombs, P. Sorgen, H.S. Duffy, S.M. Taffet, Structural bases for the chemical regulation of Connexin43 channels, Cardiovasc. Res. 62 (2004) 268–275.
[102] D. Bouvier, G. Spagnol, S. Chenavas, F. Kieken, H. Vitrac, S. Brownell, A. Kellezi, V. Forge, P.L. Sorgen, Characterization of the structure and intermolecular interactions between the connexin40 and connexin43 carboxyl-terminal and cytoplasmic loop domains, J. Biol. Chem. 284 (2009) 34257–34271.
[103] R. Grosely, F. Kieken, P.L. Sorgen, Optimizing the solution conditions to solve the structure of the connexin43 carboxyl terminus attached to the 4th transmembrane domain in detergent micelles, Cell Commun. Adhes. 17 (2010) 23–33.
[104] V.M. Unger, N.M. Kumar, N.B. Gilula, M. Yeager, Three-dimensional structure of a recombinant gap junction membrane channel, Science 283 (1999) 1176–1180.
[105] D. Locke, F. Kieken, L. Tao, P.L. Sorgen, A.L. Harris, Mechanism for modulation of gating of connexin26-containing channels by taurine, J. Gen. Physiol. 138 (2011) 321–339.

[106] B. Hille, Ion Channels of Excitable Membranes, third edition Sinauer Associates, Sunderland, MA 01375, 2001.
[107] J.T. Zhang, B.J. Nicholson, The topological structure of connexin 26 and its distribution compared to connexin 32 in hepatic gap junctions, J. Membr. Biol. 139 (1994) 15–29.
[108] M.A. Retamal, S. Yin, G.A. Altenberg, L. Reuss, Modulation of Cx46 hemichannels by nitric oxide, Am. J. Physiol. Cell Physiol. 296 (2009) C1356–C1363.
[109] C. Peracchia, L.L. Peracchia, Inversion of both gating polarity and CO_2 sensitivity of voltage gating with D3N mutation of Cx50, Am. J. Physiol. Cell Physiol. 288 (2005) C1381–C1389.
[110] J.W. Kyle, P.J. Minogue, B.C. Thomas, D.A.L. Domowicz, V.M. Berthoud, D.A. Hanck, E.C. Beyer, An intact connexin N-terminus is required for function but not gap junction formation, J. Cell Sci. 121 (2008) 2744–2750.
[111] J.-J. Tong, X. Liu, L. Dong, L. Ebihara, Exchange of gating properties between rat Cx46 and chicken Cx45.6, Biophys. J. 87 (2004) 2397–2406.
[112] L. Dong, X. Liu, H. Li, B.M. Vertel, L. Ebihara, Role of the N-terminus in permeability of chicken connexin45.6 gap junctional channels, J. Physiol. 576 (2006) 787–799.
[113] P.E. Purnick, D.C. Benjamin, V.K. Verselis, T.A. Bargiello, T.L. Dowd, Structure of the amino terminus of a gap junction protein, Arch. Biochem. Biophys. 381 (2000) 181–190.
[114] B.D. Kalmatsky, S. Bhagan, Q. Tang, T.A. Bargiello, T.L. Dowd, Structural studies of the N-terminus of Connexin 32 using ^{1}H NMR spectroscopy, Arch. Biochem. Biophys. 490 (2009) 9–16.
[115] D. Shearer, W. Ens, K. Standing, G. Valdimarsson, Posttranslational modifications in lens fiber connexins identified by off-line-HPLC MALDI-quadrupole time-of-flight mass spectrometry, Investig. Ophthalmol. Vis. Sci. 49 (2008) 1553–1562.
[116] D. Locke, S. Bian, H. Li, A.L. Harris, Post-translational modifications of connexin26 revealed by mass spectrometry, Biochem. J. 424 (2009) 385–398.
[117] B.J. Nicholson, M.W. Hunkapiller, L.B. Grim, L.E. Hood, J.P. Revel, Rat liver gap junction protein: properties and partial sequence, Proc. Natl. Acad. Sci. 78 (1981) 7594–7598.
[118] E.L. Hertzberg, R.M. Disher, A.A. Tiller, Y. Zhou, R.G. Cook, Topology of the Mr 27,000 liver gap junction protein. Cytoplasmic localization of amino- and carboxyl termini and a hydrophilic domain which is protease-hypersensitive, J. Biol. Chem. 263 (1988) 19105–19111.
[119] T.M. Suchyna, L.X. Xu, F. Gao, C.R. Fourtner, B.J. Nicholson, Identification of a proline residue as a transduction element involved in voltage gating of gap junctions, Nature 365 (1993) 847–849.
[120] W. Im, S. Seefeld, B. Roux, A Grand Canonical Monte Carlo–Brownian dynamics algorithm for simulating ion channels, Biophys. J. 79 (2000) 788–801.
[121] S.Y. Noskov, W. Im, B. Roux, Ion permeation through the alpha-hemolysin channel: theoretical studies based on Brownian dynamics and Poisson–Nernst–Plank electrodiffusion theory, Biophys. J. 87 (2004) 2299–2309.
[122] K.I. Lee, H. Rui, R.W. Pastor, W. Im, Brownian dynamics simulations of ion transport through the VDAC, Biophys. J. 100 (2011) 611–619.
[123] O.S. Smart, J.G. Neduvelil, X. Wang, B.A. Wallace, M.S. Sansom, HOLE: a program for the analysis of the pore dimensions of ion channel structural models, J. Mol. Graph. 14 (1996) 354–360 376.
[124] B. Egwolf, Y. Luo, D.E. Walters, B. Roux, Ion selectivity of alpha-hemolysin with beta-cyclodextrin adapter. II. Multi-ion effects studied with grand canonical Monte Carlo/Brownian dynamics simulations, J. Phys. Chem. B 114 (2010) 2901–2909.
[125] H. Rui, K.I. Lee, R.W. Pastor, W. Im, Molecular dynamics studies of ion permeation in VDAC, Biophys. J. 100 (2011) 602–610.
[126] H.I. Ingólfsson, Y. Li, V.V. Vostrikov, H. Gu, J.F. Hinton, R.E. Koeppe, B.t. Roux, O.S. Andersen, Gramicidin a backbone and side chain dynamics evaluated by molecular dynamics simulations and nuclear magnetic resonance experiments. I: Molecular dynamics simulations, J. Phys. Chem. B 115 (2011) 7417–7426.
[127] B. Roux, S. Bernèche, B. Egwolf, B. Lev, S.Y. Noskov, C.N. Rowley, H. Yu, Ion selectivity in channels and transporters, J. Gen. Physiol. 137 (2011) 415–426.
[128] F. Khalili-Araghi, J. Gumbart, P.-C. Wen, M. Sotomayor, E. Tajkhorshid, K. Schulten, Molecular dynamics simulations of membrane channels and transporters, Curr. Opin. Struct. Biol. 19 (2009) 128–137.
[129] A. Hung, I. Yarovsky, Gap junction hemichannel interactions with zwitterionic lipid, anionic lipid, and cholesterol: molecular simulation studies, Biochemistry 50 (2011) 1492–1504.
[130] L. Bao, F. Sachs, G. Dahl, Connexins are mechanosensitive, Am. J. Physiol. Cell Physiol. 287 (2004) C1389–C1395.
[131] J. Gullingsrud, K. Schulten, Gating of MscL studied by steered molecular dynamics, Biophys. J. 85 (2003) 2087–2099.
[132] V. Yarov-Yarovoy, D. Baker, W.A. Catterall, Voltage sensor conformations in the open and closed states in ROSETTA structural models of K(+) channels, Proc. Natl. Acad. Sci. U. S. A. 103 (2006) 7292–7297.
[133] F. Khalili-Araghi, V. Jogini, V. Yarov-Yarovoy, E. Tajkhorshid, B. Roux, K. Schulten, Calculation of the gating charge for the Kv1.2 voltage-activated potassium channel, Biophys. J. 98 (2010) 2189–2198.
[134] D.E. Shaw, M.M. Deneroff, R.O. Dror, J.S. Kuskin, R.H. Larson, J.K. Salmon, C. Young, B. Baston, K.J. Bowers, J.C. Chao, M.P. Eastwood, J. Gagliardo, J.P. Grossman, C.R. Ho, C.J. Ierardi, I. Kolossaváry, J.L. Klepeis, T. Layman, C. McLeavey, M.A. Moraes, R. Mueller, E.C. Priest, Y. Shan, J. Spengler, M. Theobald, B. Towles, S.C. Wang, Millisecond-scale Molecular Dynamics Simulations on Anton, ACM Press, New York, 2009.
[135] D.E. Shaw, P. Maragakis, K. Lindorff-Larsen, S. Piana, R.O. Dror, M.P. Eastwood, J.A. Bank, J.M. Jumper, J.K. Salmon, Y. Shan, W. Wriggers, Atomic-level characterization of the structural dynamics of proteins, Science 330 (2010) 341–346.
[136] Y. Tang, G. Cao, X. Chen, J. Yoo, A. Yethiraj, Q. Cui, A finite element framework for studying the mechanical response of macromolecules: application to the gating of the mechanosensitive channel MscL, Biophys. J. 91 (2006) 1248–1263.
[137] A.C. Pan, D. Sezer, B. Roux, Finding transition pathways using the string method with swarms of trajectories, J. Phys. Chem. B 112 (2008) 3432–3440.
[138] E.H. Lee, J. Hsin, M. Sotomayor, G. Comellas, K. Schulten, Discovery through the computational microscope, Structure 17 (2009) 1295–1306.
[139] A. Auerbach, Life at the top: the transition state of AChR gating, Sci. STKE (2003) re11.
[140] A. Auerbach, The gating isomerization of neuromuscular acetylcholine receptors, J. Physiol. 588 (2010) 573–586.
[141] D.J. Cadugan, A. Auerbach, Linking the acetylcholine receptor-channel agonist-binding sites with the gate, Biophys. J. 99 (2010) 798–807.